Energy 278 (2023) 127596

Contents lists available at ScienceDirect

Energy

journal homepage: www.elsevier.com/locate/energy

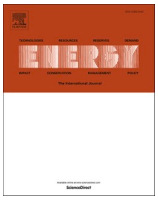

# Four approaches for the year-round operation of wood-fired heating plants with low pollutant emissions

Felix Schumacher [*,1], Thomas Nussbaumer

*Lucerne University of Applied Science and Arts, CCTEVT, Technikumstrasse 21, 6048, Horw, Switzerland*

ARTICLE INFO

Handling Editor: Henrik Lund

*Keywords:*
District heat
Wood combustion
Pollutant reduction
Thermal storage
Greenhouse gas reduction

ABSTRACT

Fluctuations in heat demand and low heat demand in summer make it difficult to operate wood boilers all year round at high efficiency and low pollutant emissions. Therefore, today's wood-fired heating plants are often equipped with an auxiliary fossil fuel boiler. This paper investigates technical approaches to operate wood heating plants without additional fossil heat while avoiding unfavorable operation with high pollutant emissions. To evaluate these concepts, the dynamic behavior of wood-fired heating plants is modelled. The model includes one to four wood boilers, an auxiliary fossil fuel boiler, the heat demand, a stratified heat storage tank and the control system. The simulation reveals that the fossil share can be eliminated by large boiler output ranges and the use of several wood boilers in cascade. High storage capacities and large boiler output ranges enable low pollutant emissions and low cool down losses of the wood boilers. By doubling the storage capacity from 30 to 60 min of the nominal boiler output, reductions of the annual emissions of carbon monoxide and particulate matter of 17% and 8% are observed. Mitigating heat demand peaks can reduce pollutant emissions of heating plants with small storage capacity.

Nomenclature

| | | |
|---|---|---|
| $e_S$ | Deviation of heat storage level and its set value | - |
| $EF_k$ | Emission factor of pollutant $k$ | mg $MJ^{-1}$ |
| $f_B$ | Control variable of the wood boiler output | -g $MJ^{-1}$ |
| $f_{bezier}$ | Setting factor for the stratification behavior in the heat storage tank | - |
| $f_{D,day}$ | Distribution function of the daily heat demand | - |
| $f_S$ | Heat storage level of the thermal storage | - |
| $f_{S,in,i}$ | Heat storage level to start-up the next wood boiler | - |
| $f_{S,out,i}$ | Heat storage level to shut-down the next wood boiler | - |
| $f_{S,set}$ | Set value of the heat storage level | - |
| $h_S$ | Height of the storage tank | m |
| $K_I$ | Integral gain of the PI controller | - |
| $K_P$ | Proportional gain of the PI controller | $s^{-1}$ |
| $n_B$ | Number of wood boilers in the heating plant | - |
| $n_T$ | Number of temperature sensors in the heat storage tank | - |
| $Q_{B,th}$ | Thermal inertia of the boiler | J |
| $Q_S$ | Stored heat in the storage tank | J |
| $Q_{S,nom}$ | Thermal storage capacity | J |
| $Q_{D,day}$ | Daily average heat demand | J |
| $Q_{D,hw}$ | Daily heat demand for hot water | J |
| $Q_{D,l}$ | Daily distribution losses of the district heating network | J |
| $Q_{D,m}$ | Daily heat demand measured at the inlet of the district heating network | J |
| $Q_{D,mc}$ | Daily heat demand measured at the connection to the consumers | J |
| $Q_{D,sh}$ | Daily heat demand for space heating | J |
| $\dot{Q}_B$ | Heat output of all boilers in the heating plant | W |
| $\dot{Q}_{B,aux}$ | Heat output of the fossil auxiliary boiler | W |
| $\dot{Q}_{B,i}$ | Heat output of the wood boiler $i$ | W |
| $\dot{Q}_{B,in,i}$ | Boiler input power | W |
| $\dot{Q}_{B,min,i}$ | Minimal heat output of the wood boiler i | W |
| $\dot{Q}_{B,nom,i}$ | Nominal heat output of the wood boiler i | W |
| $\dot{Q}_C$ | Heat demand of the consumers in the district heating network | W |
| $\dot{Q}_D$ | Heat demand of the district heating network | W |
| $\dot{Q}_{L,co}$ | Heat losses caused by cooling down the boilers | W |
| $\dot{Q}_{L,op}$ | Heat losses during boiler operation | W |
| $T_{amb}$ | Ambient temperature | °C |
| $T_A$ | Daily average ambient temperature | °C |
| $T_{A,lim}$ | Heating limit temperature | °C |
| $T_{B,op}$ | Operation temperature of the boiler | °C |
| $T_{in}$ | Supply temperature into the district heating network | °C |

(*continued on next column*)

(*continued*)

(*continued on next page*)

* Corresponding author.
*E-mail addresses:* Felix.schumacher@hotmail.com (F. Schumacher), thomas.nussbaumer@hslu.ch (T. Nussbaumer).
[1] Permanent address: Zähringerstrasse 17, 6003, Luzern, Switzerland.

https://doi.org/10.1016/j.energy.2023.127596
Received 29 November 2022; Received in revised form 21 March 2023; Accepted 18 April 2023
Available online 29 April 2023

(*continued*)

| | | |
|---|---|---|
| $T_{in,min}$ | Lowest supply temperature desired for the district heating network | °C |
| $T_{out}$ | Return temperature from the district heating network | °C |
| $T_S$ | Temperature in the heat storage tank | °C |
| $T_{S,i}$ | Temperature in the heat storage tank measured by temperature sensor $i$ | °C |
| $\Delta h$ | Height of the thermocline in the heat storage tank | mm |
| $\Delta t$ | Time step for the numerical calculations | s |
| $\gamma$ | Run variable of the stratification modulation in the heat storage tank | - |
| $\varepsilon_{a,k}$ | Annual average emission factor of the pollutant $k$ | mg $MJ^{-1}$ |
| $\eta_a$ | Annual boiler efficiency | -g $MJ^{-1}$ |
| $\eta_B$ | Boiler efficiency | - |
| $\tau_{1/2}$ | Half-life time of the boiler cooling down | s |
| $\tau_S$ | Time constant to link the storage capacity with the nominal boiler output | Min/h |
| $\tau_{th}$ | Time constant to link the thermal inertia with the nominal boiler output | s |
| $\omega$ | Inertia coefficient of the wood boilers | - |
| **Indices** | | |
| *i* | Index of boiler or temperature sensor | |
| *lim* | Limit | |
| *meas* | Measured variable | |
| *min* | Minimal | |
| *nom* | Nominal | |
| *sim* | Simulated variable | |
| * | Before limitation | |
| ** | After limitation | |

## 1. Introduction

District heating networks can make an important contribution to a fossil-free heat supply by enabling waste heat recovery, the inclusion of fluctuating renewable heat sources and the use of biomass based combined heat and power [1]. Today, 10% of the world's heat supply is provided by district heating networks [2]. However, only 9% of district heating is renewable globally and only 27% across Europe [3]. In the future, the non-renewable heat supply of district heating networks must be replaced by renewable sources. Wood-fired heating plants offer a possibility for a year-round heat supply of district heating networks without the use of fossil heat. For a sustainable operation of wood-fired heating plants, some general conditions must be met.

In today's wood heating plants, a fossil auxiliary boiler is often installed in addition to the wood boilers. The fossil auxiliary boiler supports the wood boiler during high demand peaks or replaces the wood boiler if the heat demand is below the minimum boiler output of the wood boiler. In the future, the use of fossil heat should be eliminated in wood heating plants. However, a year-round heat supply with wood boilers can lead to high pollutant emissions since the emissions from wood boilers strongly depend on their operating condition. Although the dependences of pollutant emissions on the operation conditions of different boilers vary, the following tendencies are evident: Partial load operation often causes increased emissions of carbon monoxide (CO) and unburned hydrocarbons [4–6], while nitrogen oxides are often moderately reduced during part-load operation [5,7]. Various studies have found increased CO emissions during boiler startups [8,9]. The dependence of particulate matter emissions on operating conditions is less pronounced [10]. However, depending on the technology and the type of operation, particles from incomplete combustion can potentially be increased during start-up. In addition, the effect of certain types of particle precipitators is reduced at low temperatures during boiler startup [11].

The design and control of future wood-fired heating plants should enable a year-round heat supply with wood boilers, in which the boilers are as rarely as possible in operating states with high pollutant emissions. The number of startups and shutdowns of the boilers should be kept as low as possible. In addition, the boilers should not be operated below the minimum intended boiler output. A further reduction in pollutant emissions can be achieved by flue gas treatment [12], which, however, need to be operated appropriately to avoid a reduced effect e.g. at low flue gas temperatures. In addition to pollutant emissions, heat losses must also be considered, as these also depend on the operating conditions. The heat losses of wood boilers can be divided into losses during boiler operation and cooling losses. The losses during operation include the thermal and chemical flue gas losses and the heat radiation of the boiler to the environment [13]. The cooling losses include the cooling of the thermal boiler mass after the boiler has been switched off [14].

Over the past decades, various studies have confirmed that heat storage can have a positive effect on the operation of wood-fired heating plants. Heat storage balances heat demand fluctuations and thus can prevent unnecessary boiler startups, which reduces pollutant emissions and increases efficiencies [15–19]. Various studies in recent years have also shown that the operation of wood-fired heating plants can be improved by intervening on the demand side. [20] summarizes the results of various publications on thermal load management of district heating networks. By mitigating load peaks, the demand for primary energy could be reduced by up to 5%. In Ref. [21], the control behavior of various wood-fired heating plants was investigated. In all plants, undesirable operating states were found, which were caused by strongly pronounced and partly avoidable demand peaks.

The present work investigates and compares the influence of different measures on a year-round heating plant operation. In contrast to the available studies, all influences are clearly assigned to an operating state (stationary or transient). Pollutant emissions, plant efficiency and the use of fossil fuel are considered in all analyses. In addition to storage capacity and load management, this work examines two other measures that have not yet been considered in the scientific papers yet.

1. Integration of a thermal storage tank into the heating plant.
2. Mitigation of peak heat demand through thermal load management.
3. The use of boilers with a large boiler output range, i.e. boilers that can be operated between a low minimal boiler output and its rated output.
4. The use of wood boiler cascades in the wood heating plant.

In this work, the dynamic year-round operation of wood heating plants is simulated. The model can represent wood heating plants with several wood boilers in combination with a fossil auxiliary boiler and a stratified heat storage tank. The dynamic heat demand is derived from the measured heat demand of a district heating network in Switzerland. In addition to the thermodynamic processes, the control processes are also considered, as these have a major influence on the operation of wood heating plants. Various simulations are carried out, in which the following measures were varied: Storage capacity, mitigation of peak demand, wood boiler output range and number of wood boilers. The simulation results are evaluated and compared with experimental data from a storage tank in a laboratory and a district heating network supplied by a cascade of wood boilers. The fossil share of the heat supply or the fossil $CO_2$ emissions, the annual heat losses and the pollutant emissions of carbon monoxide (CO), nitrogen oxides ($NO_X$) and particulate matter (PM) serve as evaluation variables.

The approach of the model is a further development of an existing model that was used for the optimization of control concepts of wood heating plants with a single wood boiler and a stratified storage tank [22]. The approach is described in chapter 2, validated in chapter 3.1. The simulation results with focus on the fossil share, pollutant emissions and heat losses are shown in the chapters 4.1, 4.2 and 4.3. In chapter 4.4 all the simulation results are summarized in tables.

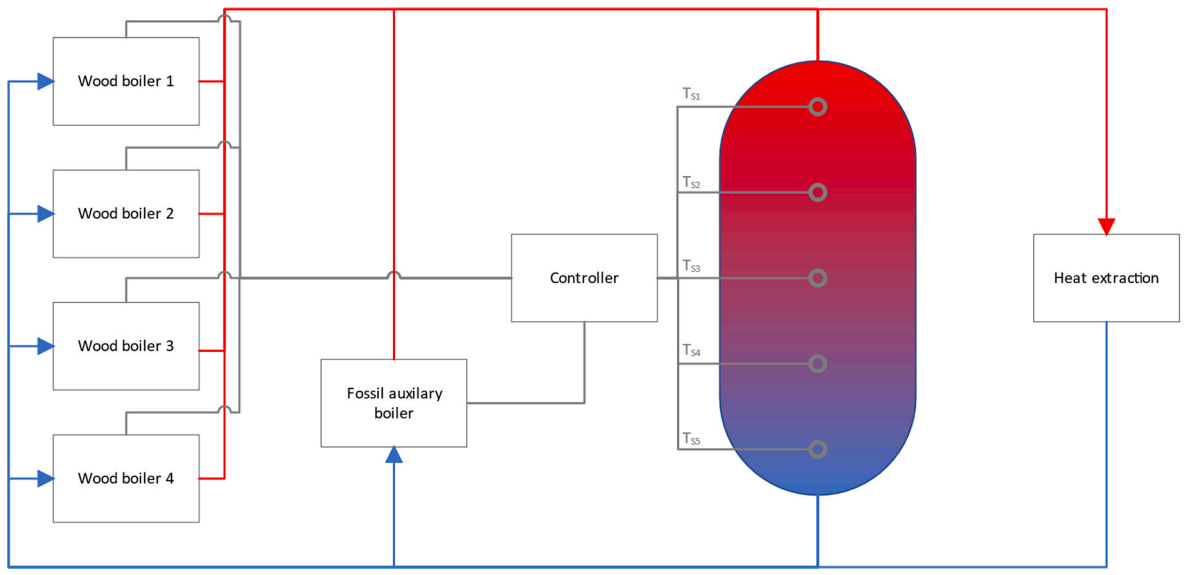


**Fig. 1.** Flow diagram of the model. Blue lines: Return lines with low temperature. Red lines: Supply lines with high temperature. Grey lines: Signals from the temperature measurement in the heat storage tank and control signals from the controller to the boilers. $T_{S1}$ to $T_{S5}$ represent the temperature measurements in the heat storage tank.

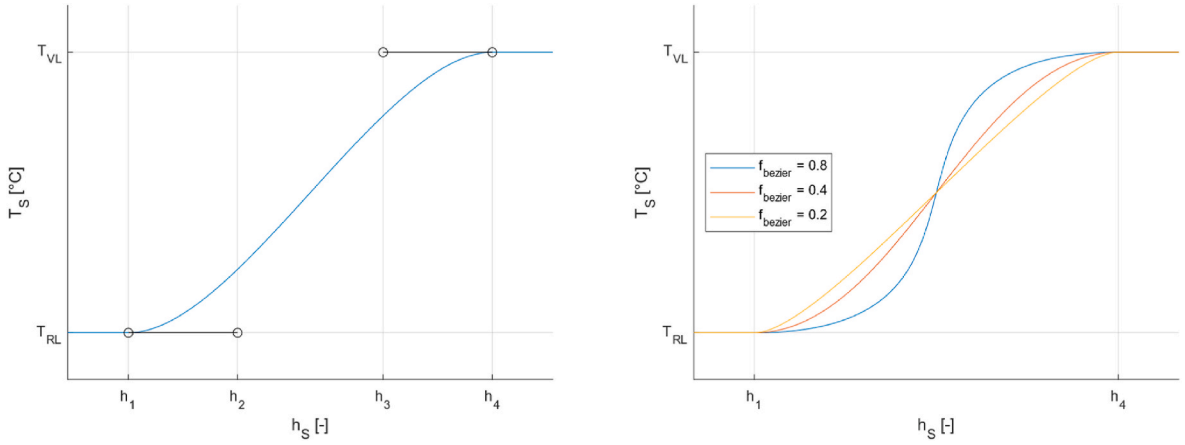


**Fig. 2.** Modelling of the temperature curve in the thermocline using Bézier curves.

## 2. Procedure

### 2.1. Overview of the model

The model describes the thermodynamic and control processes in a wood-fired heating plant during dynamic heat extraction. The structure of the model is illustrated in Fig. 1. The model includes heat generation with any number of wood boilers and a fossil auxiliary boiler, a stratified heat storage tank with any storage capacity, a dynamic heat extraction and a controller with a choice of different control approaches. The heat extraction represents the heat demand of an individual heat consumer or an entire heat network for up to one year. The heat storage tank is intended to compensate for short-term differences between the heat demand and the heat production. The controller observes the heat storage level of the storage tank via any number of temperature sensors evenly distributed over the tank height and attempts to minimize the deviation of the heat storage level and its set point via output modulation of the boilers and switching on and off the boilers .

### 2.2. Model of the heat storage tank

The stored heat in the heat storage tank $Q_S$ is calculated by an energy balance over the heat storage tank [1]. Temporal changes of $Q_S$ are caused by deviations of the heat supplied by the boilers $\dot{Q}_B$ and the heat extraction of the heating network $\dot{Q}_D$.

$$\frac{\partial Q_S}{\partial t} = \dot{Q}_B - \dot{Q}_D \tag{1}$$

The heat output supplied by the boilers corresponds to the sum of all wood boiler outputs $\dot{Q}_{B,i}$ and the boiler output of the fossil auxiliary boiler $\dot{Q}_{B,aux}$ [2].

$$\dot{Q}_B = \dot{Q}_{B,aux} + \sum_{i=1}^{n_B} \dot{Q}_{B,i} \tag{2}$$

The amount of heat stored in the heat storage tank is limited by the storage capacity $Q_{S,nom}$ [3].

$$0 \leq Q_S \leq Q_{S,nom} \tag{3}$$

The storage capacity is specified the time constant $\tau_S$ which indicates

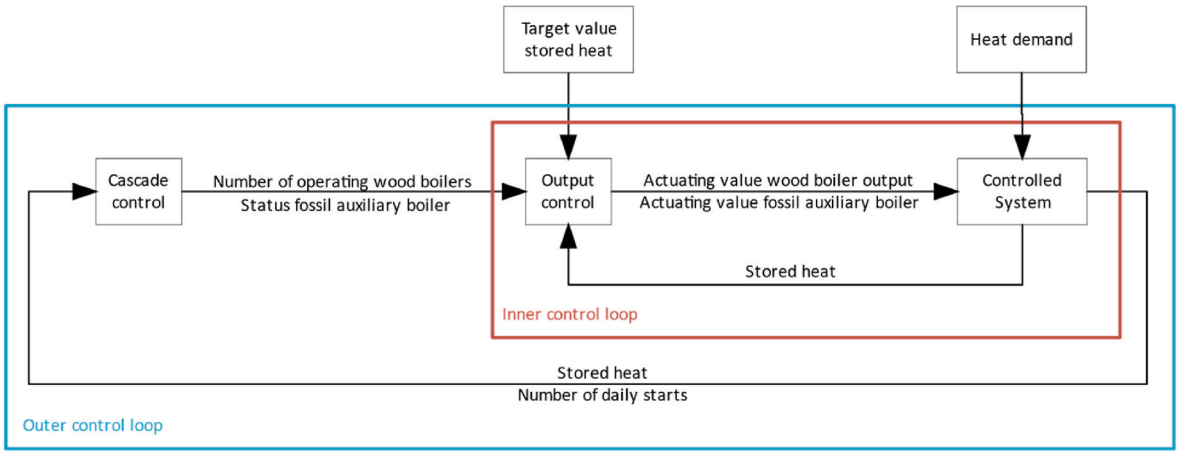


**Fig. 3.** Structure of the control system.

**Table 1**
Start-up conditions related to the heat storage level.

| | Boiler 1 | Boiler 2 | Boiler 3 | Boiler 4 |
|---|---|---|---|---|
| 1-boiler plant | 50% | | | |
| 2-boiler plant | 67% | 33% | | |
| 3-boiler plant | 75% | 50% | 25% | |
| 4-boiler plant | 80% | 60% | 40% | 20% |

**Table 2**
Shut-down conditions related to the heat storage level.

| | Boiler 1 | Boiler 2 | Boiler 3 | Boiler 4 |
|---|---|---|---|---|
| 1-boiler plant | 100% | | | |
| 2-boiler plant | 100% | 90% | | |
| 3-boiler plant | 100% | 90% | 80% | |
| 4-boiler plant | 100% | 90% | 80% | 70% |

the ratio of the storage capacity to the sum of the installed wood boiler outputs $\dot{Q}_{B,nom,i}$ [4].

$$Q_{S,nom} = \tau_S \bullet \sum_{i=1}^{n_B} \dot{Q}_{B,nom,i} \tag{4}$$

The heat storage level represents the ratio of the stored heat to the storage capacity [5].

$$f_S = \frac{Q_S}{Q_{S,nom}} \tag{5}$$

When the upper limit is reached (storage tank full), the boilers must be switched off to prevent the storage tank and the boilers from overheating. When the lower limit is reached (storage tank empty), the storage tank cannot provide any heat output to cover the heat demand. If the heat demand with an empty storage tank is higher than the supplied boiler output, a heat deficit arises that should be covered as quickly as possible. In the model, the heat deficit is taken into account by differentiating between the heat demand of the consumers $\dot{Q}_C$ and the heat demand of the heating network $\dot{Q}_D$. The heat demand of the consumers is independent of the operation of the heating plant. The heat output demand of the heating network, on the other hand, considers uncovered heat output demand from the past [6].

$$\dot{Q}_D(t) = \dot{Q}_D(t-1) + \dot{Q}_B(t-1) - \frac{Q_S(t) - Q_S(t-1)}{\Delta t} - \dot{Q}_C(t-1) \tag{6}$$

The model represents a stratified tank. When the stratified tank is loaded, hot water at supply temperature $T_{in}$ flows from the top into the stratified tank while cold water at the heating network return temperature $T_{out}$ leaves the storage tank at the bottom. Discharge proceeds the other way round. A warm layer forms at the top of the storage tank, a cold layer at the bottom and a thermocline in between, in which the temperature drops from the supply temperature to the return temperature from top to bottom. The course of the storage tank temperature $T_S$ over the storage tank height $h_S$ is calculated using a Bézier curve (Fig. 2). The temperature profile can be adjusted with the thermocline width $\Delta h$ and the setting factor $f_{bezier}$ to the stratification behavior of a specific storage tank. The resolution of the temperature profile is determined by the resolution of the run variable $\gamma$ [13]. Equation [7] provides the temperature in the storage tank at the height, given by Refs. [8–12].

$$T_{S,\gamma} = \left[(1-\gamma)^3 + 3 \bullet (1-\gamma)^2 \bullet \gamma\right] \bullet T_{out} + \left[3 \bullet (1-\gamma) \bullet \gamma^2 + \gamma^3\right] \bullet T_{in} \tag{7}$$

$$h_{S,\gamma} = (1-\gamma)^3 \bullet h_1 + 3 \bullet (1-\gamma)^2 \bullet \gamma \bullet h_2 + 3 \bullet (1-\gamma) \bullet \gamma^2 \bullet h_3 + \gamma^3 \bullet h_4 \tag{8}$$

$$h_1 = f_S - \frac{\Delta h}{2} \tag{9}$$

$$h_2 = f_S - \frac{\Delta h}{2} + f_{bezier} \bullet \Delta h \tag{10}$$

$$h_3 = f_S + \frac{\Delta h}{2} - f_{bezier} \bullet \Delta h \tag{11}$$

$$h_4 = f_S + \frac{\Delta h}{2} \tag{12}$$

$$0 \le \gamma \le 1 \tag{13}$$

### 2.3. Model of the control system

The control system consists of two control loops (Fig. 3). The outer control loop (cascade control) decides how many wood boilers are needed to cover the heat demand and issues startup and shutdown commands to the individual wood boilers. In addition, the outer control loop decides whether the fossil auxiliary boiler is needed. The inner control loop (output control) controls the heat outputs of the individual wood boilers in the operating state.

The model of the cascade control system is based on the observations of a field investigation, which examines the operation of wood-fired heating plants with several wood boilers in practice [21]. The cascade control system uses a list of start-up or shut-down conditions related to the heat storage level, to decide whether a start or stop command is needed. The start-up or shut-down conditions depend on the number of installed wood boilers, can be calculated with [14,15] and are listed in

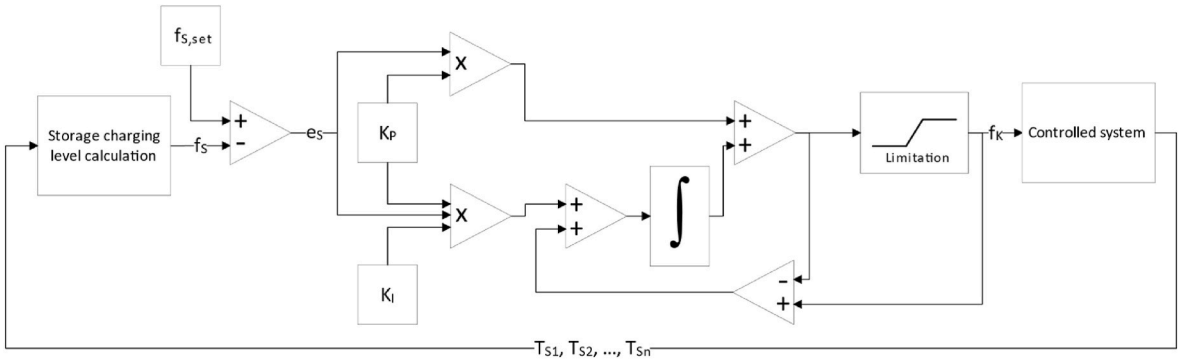


**Fig. 4.** Structure of the inner control loop (output control).

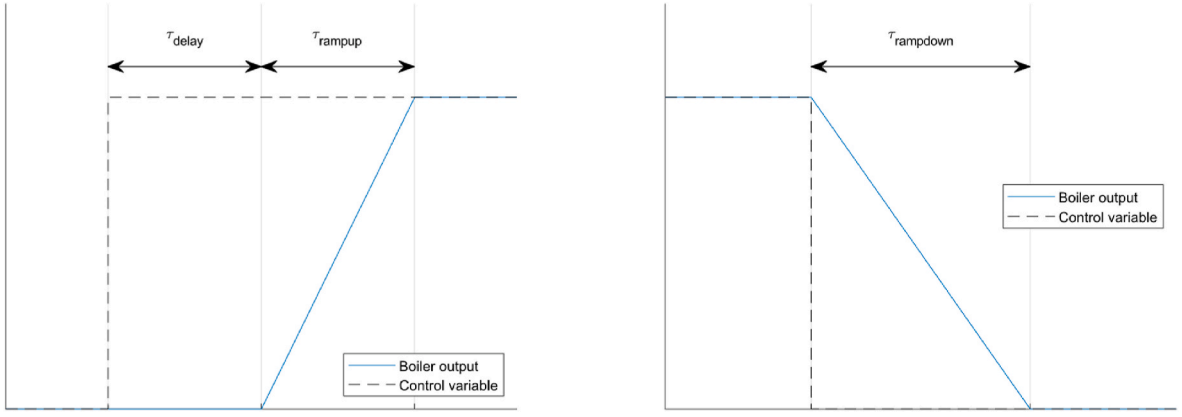


**Fig. 5.** Boiler dynamics during cutting-in or cutting-out a wood boiler.

Table 1 and Table 2 for heating plants with one to four wood boilers.

$$f_{S,in,i} = 1 - \frac{i}{n_K + 1} \tag{14}$$

$$f_{S,out,i} = 1 - \frac{i-1}{10} \tag{15}$$

The output control defines the output of the individual wood boilers by the control variable $f_B$ [16]. $\dot{Q}^*_{B,i}$ represents the boiler output, where the inertia of the systems response is not considered yet. The outputs of the wood boilers are limited by their minimal and nominal output [17], therefore the control variable $f_B$ is limited [18]. To consider the thermal inertia of the wood boilers, the time derivative of the control variable $f_B$ is limited too [19]. The control variable is calculated by a PI controller [20]. The PI controller minimizes the deviation $e_S$ of the heat storage level $f_S$ and its set value $f_{S,set}$ [21]. $f^*_B$ represents the control variable before limitation. $K_P$ and $K_I$ represent the proportional and the integral gain. The integral windup caused by the control variable limitation is addressed by a backward calculation anti windup approach [23]. The structure of the output control is shown in Fig. 4.

$$\dot{Q}^*_{B,i} = \dot{Q}_{B,min,i} + f_K \bullet \left(\dot{Q}_{B,\mathrm{nom},i} - \dot{Q}_{B,min,i}\right) \tag{16}$$

$$\dot{Q}_{B,min,i} \le \dot{Q}_{B,i} \le \dot{Q}_{B,\mathrm{nom},i} \tag{17}$$

$$0 \le f_B \le 1 \tag{18}$$

$$\frac{\partial f_B}{\partial t} \le \left[\frac{\partial f_B}{\partial t}\right]_{max} \tag{19}$$

$$f^*_B(t) = K_P \bullet \left[e_S(t) + K_I \bullet \sum\nolimits_{\tau=0}^{t} e_S(\tau) + f_B(\tau) - f^*_B(\tau)\right] \tag{20}$$

$$e_S = f_{S,set} - f_S \tag{21}$$

The heat storage level $f_S$ is calculated from the temperature measurements $T_{S,i}$ in the storage tank [23]. The number of temperature sensors amounts $n_T$. The sensors are evenly distributed over the height of the storage tank. For the calculation of the heat storage level, the measured temperatures are limited by a temperature range [22]. $T_{in,min}$ marks the lowest inlet temperature of the district heating network at which the district heating network can be operated. $T_{in}$ marks the desired inlet temperature in the district heating network. $T^{**}_{S,i}$ represents the measured temperature $T_{S,i}$ after the limitation [21].

$$T_{in,min} \le T_{S,i} \le T_{in} \tag{22}$$

$$f_S = \frac{\sum_{i}^{n_T} \frac{T^{**}_{S,i} - T_{in,min}}{T_{in} - T_{in,min}}}{n_T} \tag{23}$$

The model considers delay and inertia in the output control. The systems response of the wood boilers is modelled as a serial linking of a proportional amplification and two delay elements [24]. For simplicity, two identical delay elements are used [24]. $\dot{Q}^*_{B,i}$ is the wood boiler output set by the controller without considering delay and inertia. $\dot{Q}_B$ is the delayed wood boiler output. $t_0$ marks the time where the control variable changes. The coefficient ω can calculated by the method of least squares from the measurement results.

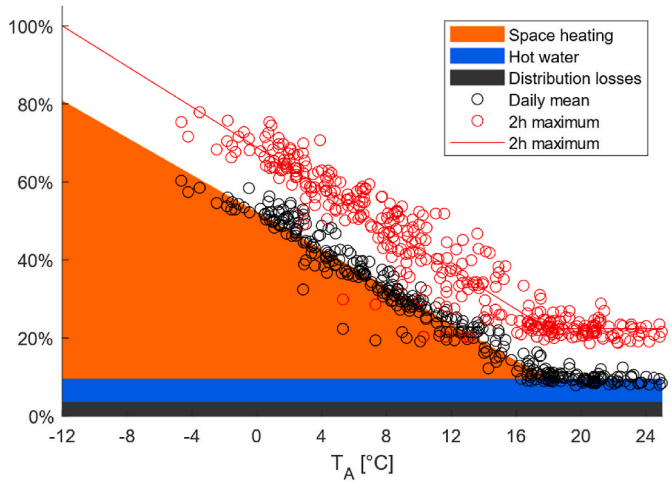


**Fig. 6.** Stacked characteristic curve of the average daily heat demand as a function of the daily average ambient temperature. The mean daily heat demand refers to the total installed boiler output in %. The dots mark the demand measurements in the district heating network on which the model is based.

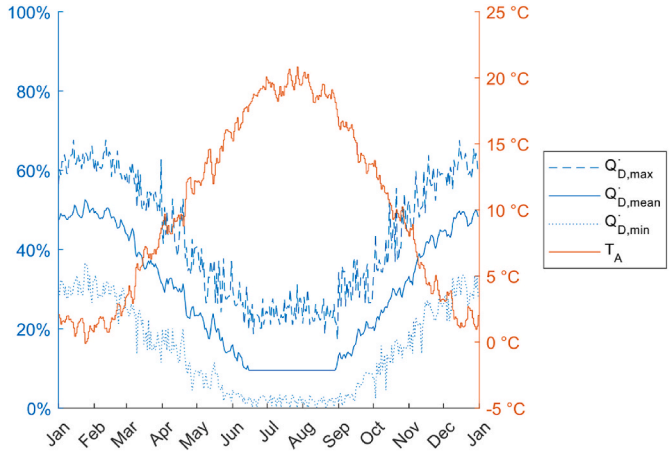


**Fig. 7.** Simulation results of the annual course of the heat demand (left y-axis) depending on the average daily temperature (right y-axis). The heat demand refers to the total installed boiler output in %. The solid blue line represents the daily average of the heat output demand, while the broken lines represent the 2-h maximum and minimum.

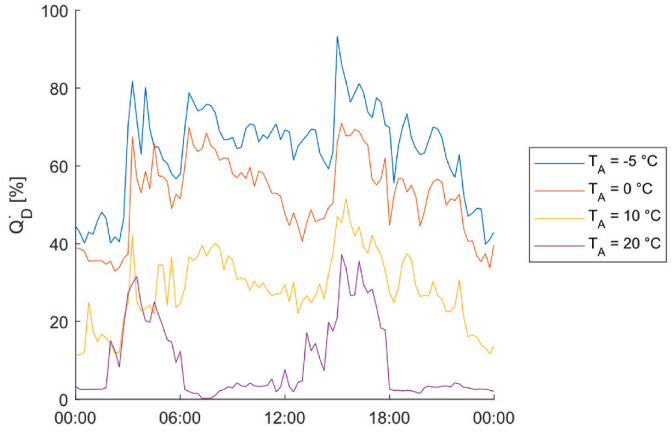


**Fig. 8.** Simulation results of daily heat demand profiles for different ambient temperatures $T_A$. The heat demand refers to the total installed boiler output in %.

**Table 3**
Constants for the calculations of the thermal losses.

| Variable | Value | Source |
|---|---|---|
| $\eta_B$ | 90% | [8] |
| $T_{B,op}$ | 80 °C | [9] |
| $T_{amb}$ | 25 °C | [7] |
| $\tau_{1/2}$ | 10 h | |
| $\tau_{th}$ | 15 min | |

**Table 4**
Emission factors for CO, PM, $NO_X$ and non-renewable $CO_2$ for the wood boilers and the fossil auxiliary boilers in mg per MJ fuel input. For wood boilers, data for category 16 an according to the statistical data on wood energy in Switzerland are considered, which comprise automated wood chip boilers greater than 500 kW which are commonly smaller than 10 MW and equipped with electrostatic precipitators [10].

| Fuel | Pollutant | CO | PM | $NO_X$ | $CO_2$ | Source |
|---|---|---|---|---|---|---|
| | | mg/MJ | mg/MJ | mg/MJ | g/MJ | – |
| Wood boiler | Start-up | 684.7 | 50.0 | 181.8 | | [10] |
| | Shut-down | 1209.1 | 50.0 | 139.4 | | |
| | Full load | 45.4 | 10.0 | 124.7 | | |
| | Part load | 64.2 | 2.8 | 104.2 | | |
| Light fuel oil boiler | Operation | 10 | 0.2 | 33 | 73.7 | [11] |
| Natural gas boiler | Operation | 8 | 0.1 | 19 | 56.4 | |

$$\frac{\dot{Q}_B(t) - \dot{Q}^*_{B,i}(t_0)}{\dot{Q}^*_{B,i}(t) - \dot{Q}^*_{B,i}(t_0)} = 1 - e^{-\omega t} \bullet (1 + \omega t) \tag{24}$$

Furthermore, dynamic behavior during start-up and shut-down processes of wood boilers is considered. During start-up of a wood boiler, the boiler output is modelled as a delay followed by a ramp. Cutting-out is modelled as a ramp without a delay Fig. 5.

### 2.4. Model of the fossil auxiliary boiler

The fossil auxiliary boiler supplements the wood boilers in the event of rapid demand changes while the storage is empty and replaces the wood boilers as soon as the low-load condition is not met. Low-load condition means that the daily heat demand should be above a limit value, to avoid boiler cycling. Boiler cycling means providing a low boiler output by frequent startups and shutdowns of the wood boiler. In the model, the low load limit value corresponds to a heat quantity which one wood boiler provides when operated during 12 h at its minimum continuous output [25]. If the daily heat demand is lower than the limit value, the heat demand of this day is covered by the fossil auxiliary boiler and the wood boilers are shut down during this day.

### 2.5. Model of the heat demand

The model examines the year-round behavior of wood heating plants with one or more wood boilers. Thus, a curve of the heat demand over a whole year is required. The dynamic heat demand is derived on an hourly basis from the measured heat demand of a district heating network in Switzerland and modelled in three steps [26].

1. A characteristic load curve is derived to show the relationship between the daily average ambient temperature $T_A$ and the daily heat demand $Q_{D,day}$ [25].

$$Q_{D,day} = f(T_A) \tag{25}$$


**Fig. 9.** Schematic view of a typical moving grate boiler (left, source: Schmid AG) and photography of the 150 kW test plant investigated in the laboratory at the Lucerne University of Applied Sciences (LUAS) (right, source: LUAS) used in the validation process.

2. Distribution functions $f_{D,day}$ [26] are derived to specify at what time during the day the heat is needed. The daily course of the heat demand and therefore the distribution function depends on $T_A$. The distribution function is a vector that defines the fraction of the daily heat demand for each timestep of the day.

$$f_{D,day} = f(t, T_A) \tag{26}$$

3. The daily course of the heat demand $\dot{Q}_D$ can be calculated for a given daily average ambient temperature $T_A$ [27].

$$\dot{Q}_D = \frac{f_{D,day}(t, T_A) \bullet Q_{D,day}(T_A)}{\Delta t} \tag{27}$$

A characteristic load curve was derived to show the relationship between the daily average ambient temperature $T_A$ and the daily heat demand $Q_{D,day}$. Therefore, the demand $Q_{D,day}$ is divided into space heating $Q_{D,sh}$, hot water $Q_{D,hw}$ and heat distribution losses of the district heating network $Q_{D,l}$ [28]. Hot water and distribution losses are considered as independent on the ambient temperature. The heat load linearly depends on the ambient temperature [27].

$$Q_{D,day} = Q_{D,sh} + Q_{D,hw} + Q_{D,l} \tag{28}$$

The distribution losses of the district heating network can be calculated by comparing the measured heat delivered into the network $Q_{D,m}$ and the heat delivered to the customers $Q_{D,mc}$ [29].

$$Q_{D,l} = Q_{D,m} - Q_{D,mc} \tag{29}$$

The daily heat demand for space heating and hot water can be calculated by linear regression. For space heating only days with an ambient temperature lower than the heating limit $T_{A,lim}$ are considered.

The distribution function $f_{D,day}$ [30] is found by dividing the measured heat demand of each timestep for one day $Q_{D,meas,t}$ by the measured daily heat demand $Q_{B,meas,day}$. To get the thermal power of the timestep $t$, the fraction is divided by the period of the timestep $\Delta t$.

$$f_{B,day} = \frac{Q_{D,meas,t}}{Q_{D,meas,day}} \tag{30}$$

Fig. 6 shows measured data (dots) of the daily heat demand as a function of the daily mean ambient temperature for the district heating network which is investigated as example for the model. The yearly course of the heat demand is shown in Fig. 7. The daily courses of four example days with different ambient temperatures are shown in Fig. 8.

### 2.6. Model of the heat losses

The heat losses of the wood boilers are divided into operating losses and cooling losses [28]. Operating losses $\dot{Q}_{L,op}$ occur during normal operation of the wood boiler and are described by the boiler efficiency $\eta_B$ [31].

$$\dot{Q}_{L,op} = (1 - \eta_B) \bullet \dot{Q}_B \tag{31}$$

Cooling losses $\dot{Q}_{L,co}$ occur due to the cooling of the thermal mass of the wood boilers after being switched off. During the cool-down phase, the temperature of the boiler mass drops exponentially from the operating temperature $T_{B,op}$ to ambient temperature $T_{amb}$. $t_0$ represents the time when the boiler is switched off and $\tau_{1/2}$ is the half-life of the cooling down (32).

$$T_B(t) = T_{amb} + \left(T_{B,op} - T_{amb}\right) \bullet e^{\frac{log(1/2)}{\tau_{1/2}} \bullet (t - t_0)} \tag{32}$$

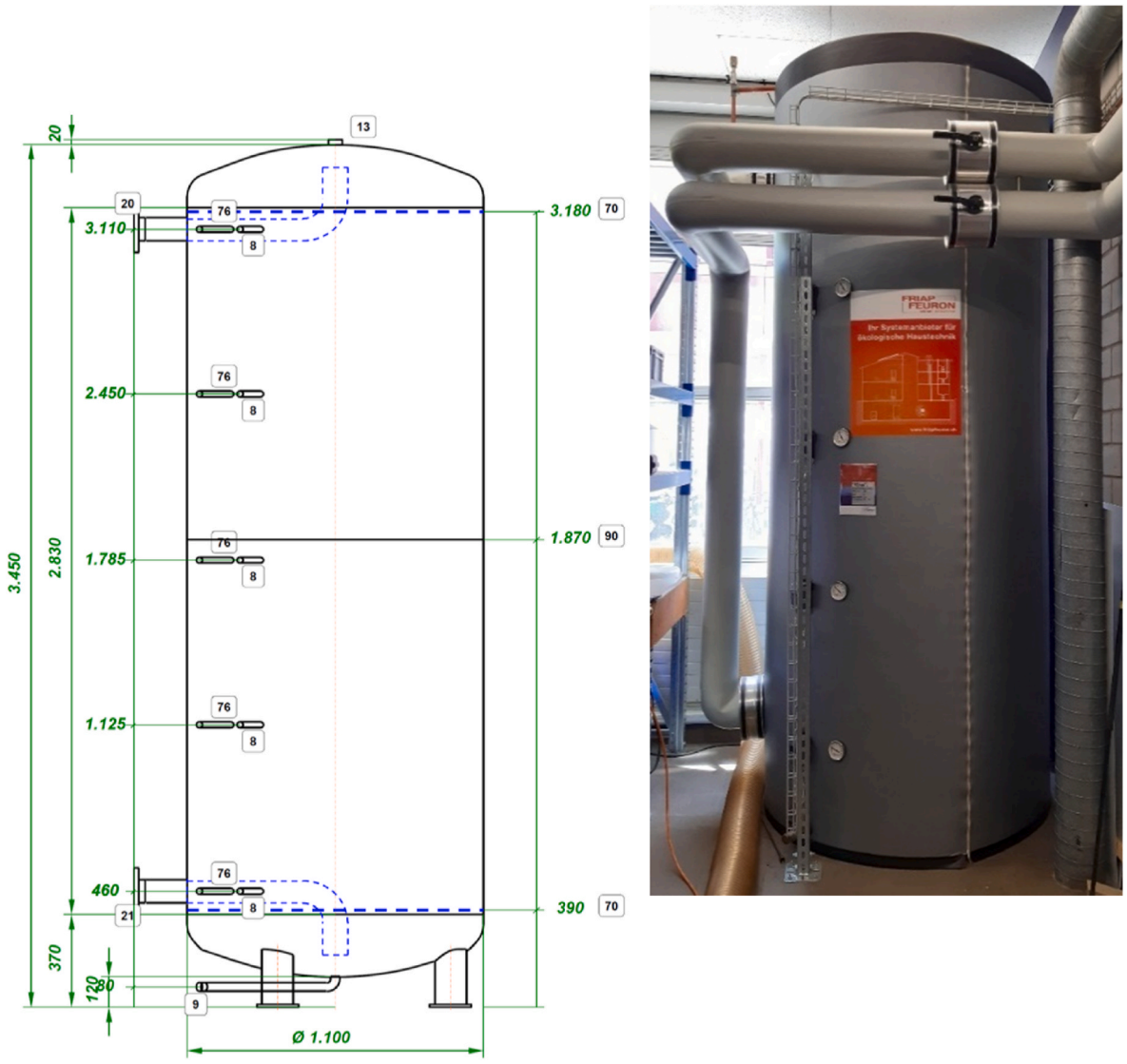


**Fig. 10.** Technical drawing with the sensor positions (left) and photography (right) of the stratified 3030 L storage tank used in the validation process.

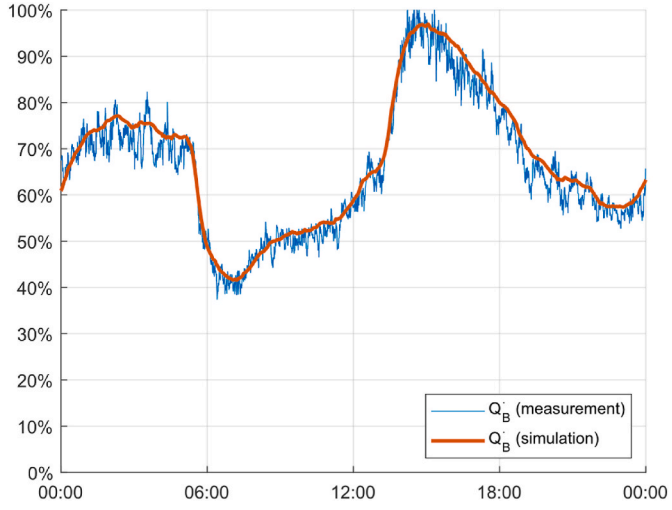


**Fig. 11.** Comparison of the measured (blue line) and simulated boiler output (red line) of a wood heating plant with a single wood boiler and a stratified storage tank for one day.

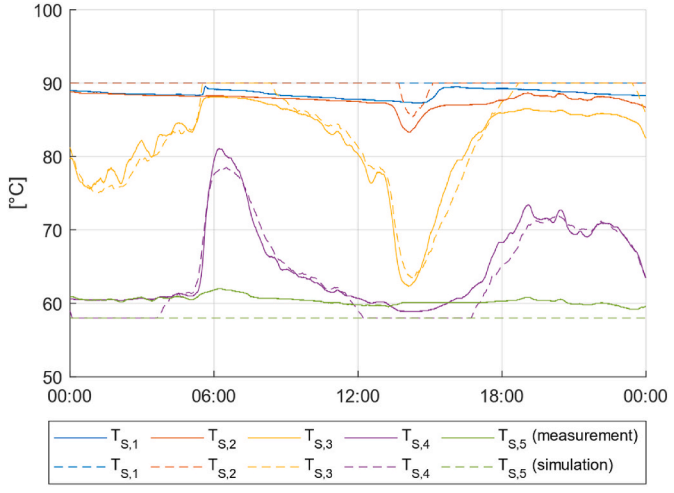


**Fig. 12.** Comparison of the measured (solid lines) and simulated temperatures in the heat storage tank (dashed lines) of a wood heating plant with a single wood boiler and a stratified storage tank for one day.

**Table 5**
Error norms of the validation process for the three test runs, that lasted 24 h each.

| | $\|\dot{Q}_B\|_2$ | $\|\dot{Q}_B\|_{Max}$ | $\|T_S\|_2$ | $\|T_S\|_{Max}$ |
|---|---|---|---|---|
| Day 1 | 3.2% | 7.5% | 2.1 K | 4.4 K |
| Day 2 | 3.2% | 12.0% | 2.9 K | 9.3 K |
| Day 3 | 3.6% | 8.7% | 2.0 K | 4.4 K |

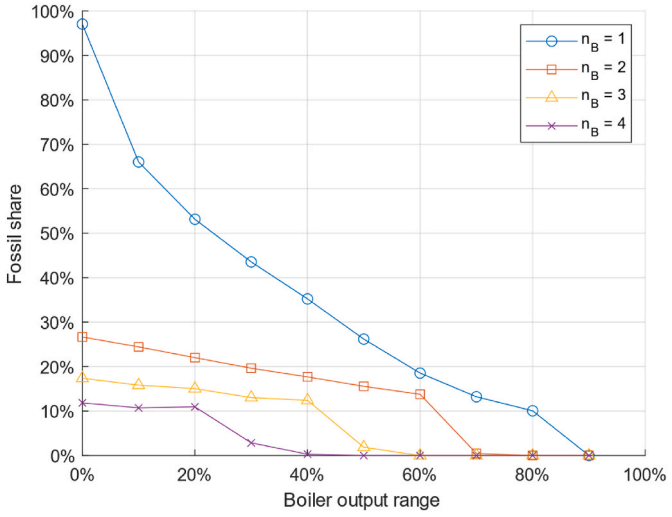


**Fig. 13.** Annual fossil share of wood heating plants with one to four wood boilers and a fossil auxiliary boiler as function of the boiler output ranges. The boiler output range is varied in 10% steps. Example: A boiler with 30% boiler output range enables output modulation from 70% to 100% of the nominal heat output.

**Table 6**
Annual fossil share of wood heating plants with one to four wood boilers and a fossil auxiliary boiler for different boiler output ranges.

| Boiler output range | Minimal and nominal boiler output | Number of wood boilers | | | |
|---|---|---|---|---|---|
| | | 1 | 2 | 3 | 4 |
| 0% | 100% | 97% | 27% | 17% | 12% |
| 10% | 90%–100% | 66% | 24% | 16% | 11% |
| 20% | 80%–100% | 53% | 22% | 15% | 11% |
| 30% | 70%–100% | 44% | 20% | 13% | 3% |
| 40% | 60%–100% | 35% | 18% | 12% | 0% |
| 50% | 50%–100% | 26% | 16% | 2% | 0% |
| 60% | 40%–100% | 19% | 14% | 0% | 0% |
| 70% | 30%–100% | 13% | 0% | 0% | 0% |
| 80% | 20%–100% | 10% | 0% | 0% | 0% |
| 90% | 10%–100% | 0% | 0% | 0% | 0% |

The heat output $\dot{Q}_{L,co}$ when cooling down can be calculated by the heat $Q_{B,th}$ stored in the boiler mass (thermal mass) and the change in boiler temperature over time (33).

$$\dot{Q}_{L,co} = \frac{\frac{\partial T_B}{\partial t}}{T_{B,op} - T_{amb}} \bullet Q_{B,th} \tag{33}$$

The thermal mass of a wood boiler is given relative to the nominal boiler output by the time constant $\tau_{th}$(34). The time constant can be interpreted as the time needed to operate the boiler at nominal load in order to bring the entire boiler mass to operating temperature.

$$Q_{B,th} = \dot{Q}_{B,nom} \bullet \tau_{th} \tag{34}$$

The input power $\dot{Q}_{B,in,i}$ of the wood boiler $i$ is calculated by adding the heat losses to the boiler output (35).

$$\dot{Q}_{B,in,i} = \dot{Q}_{B,i} + \dot{Q}_{L,op,i} + \dot{Q}_{L,co,i} \tag{35}$$

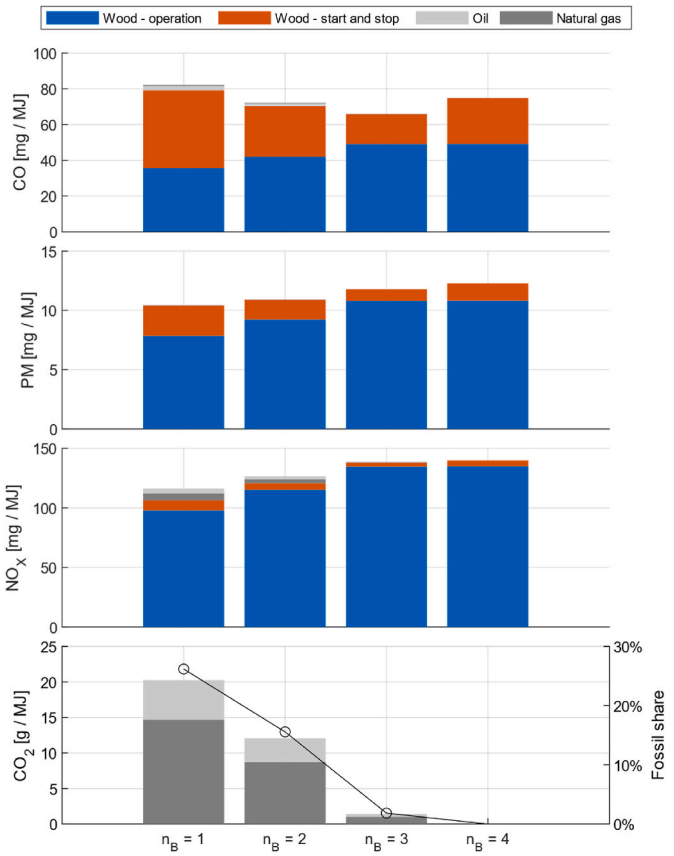


**Fig. 14.** Annual pollutant emissions of wood heating plants with one to four wood boilers ($n_B$), a fossil auxiliary boiler, a boiler output range of 50% and a heat storage of 1 h "Wood operation": operation of wood boilers without startups and shutdowns. "Wood start and stop": Transient operation during startup and shutdown.

The annual efficiency describes the ratio between the useful heat of the boiler and the supplied energy in one year (36). The useful heat corresponds to the time integral of the boiler output. The supplied heat corresponds to the time integral of the boiler output and the heat losses.

$$\eta_a = \frac{\int_{t_0}^{t_0+\tau_a} \sum_{i=1}^{n_K} \dot{Q}_{B,i}\, dt}{\int_{t_0}^{t_0+\tau_a} \sum_{i=1}^{n_K} \dot{Q}_{B,in,i}\, dt} \tag{36}$$

The assumptions for the parameters used for the simulation are introduced in Table 3.

### 2.7. Model of the pollutant emissions

The model calculates emissions of CO, PM, $NO_X$ and non-renewable $CO_2$. In the present work, wood is considered as a renewable fuel thanks to a sustainable forestry. Consequently, $CO_2$ emissions from the fossil fuel boiler are solely considered. The fossil auxiliary fuel boiler is operated with light fuel oil or natural gas. The impact on local air pollution is considered by the emissions of carbon monoxide (CO), particulate matter (PM) and nitrogen oxides ($NO_X$) of the wood boilers and the auxiliary boiler. The model of pollutant emissions is based on emission factors, listed in Table 4. In the case of wood boilers, data for

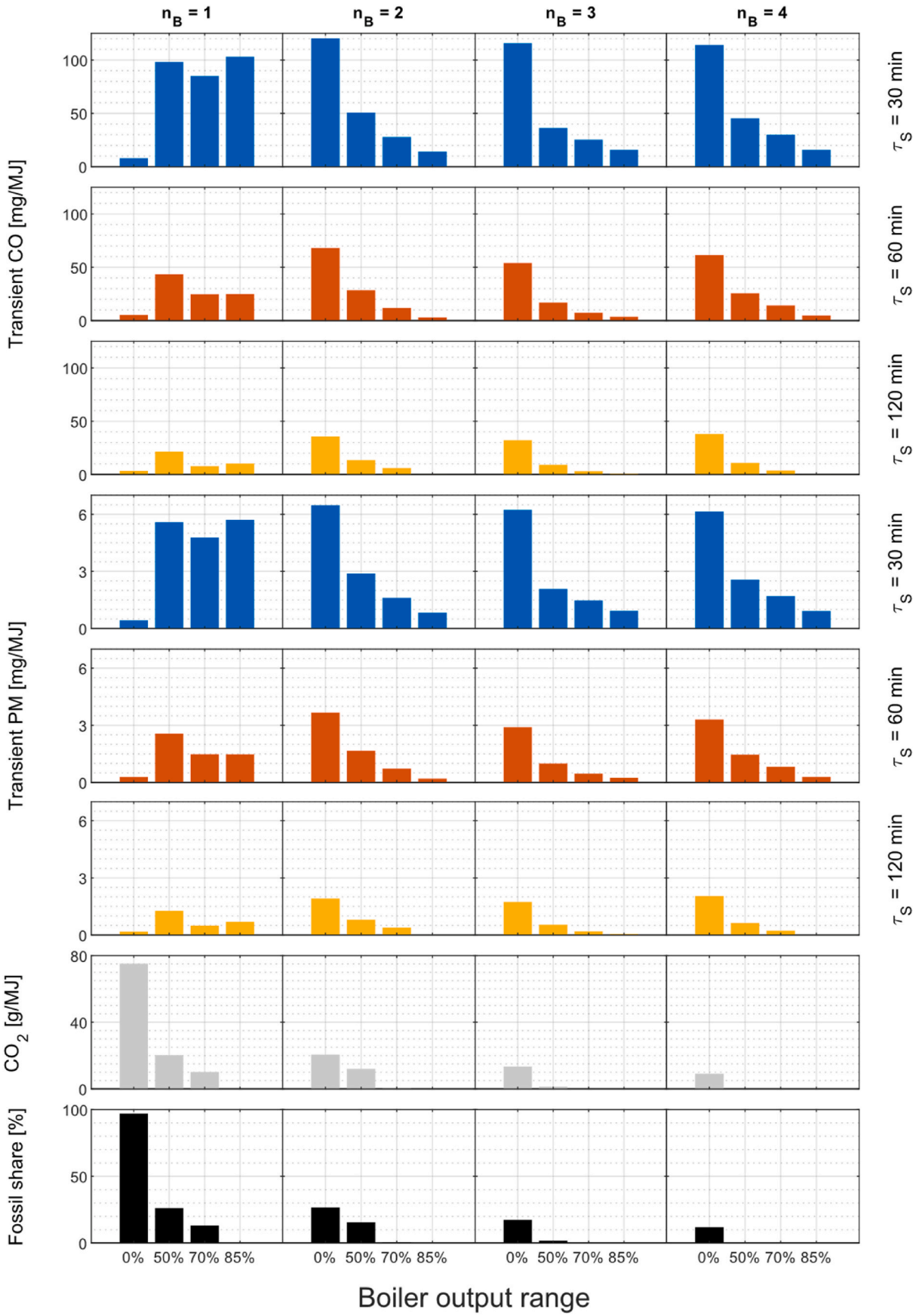


**Fig. 15.** Annual pollutant emissions during the transient operation of wood heating plants with one to four wood boilers and a fossil auxiliary boiler operated with light fuel oil.

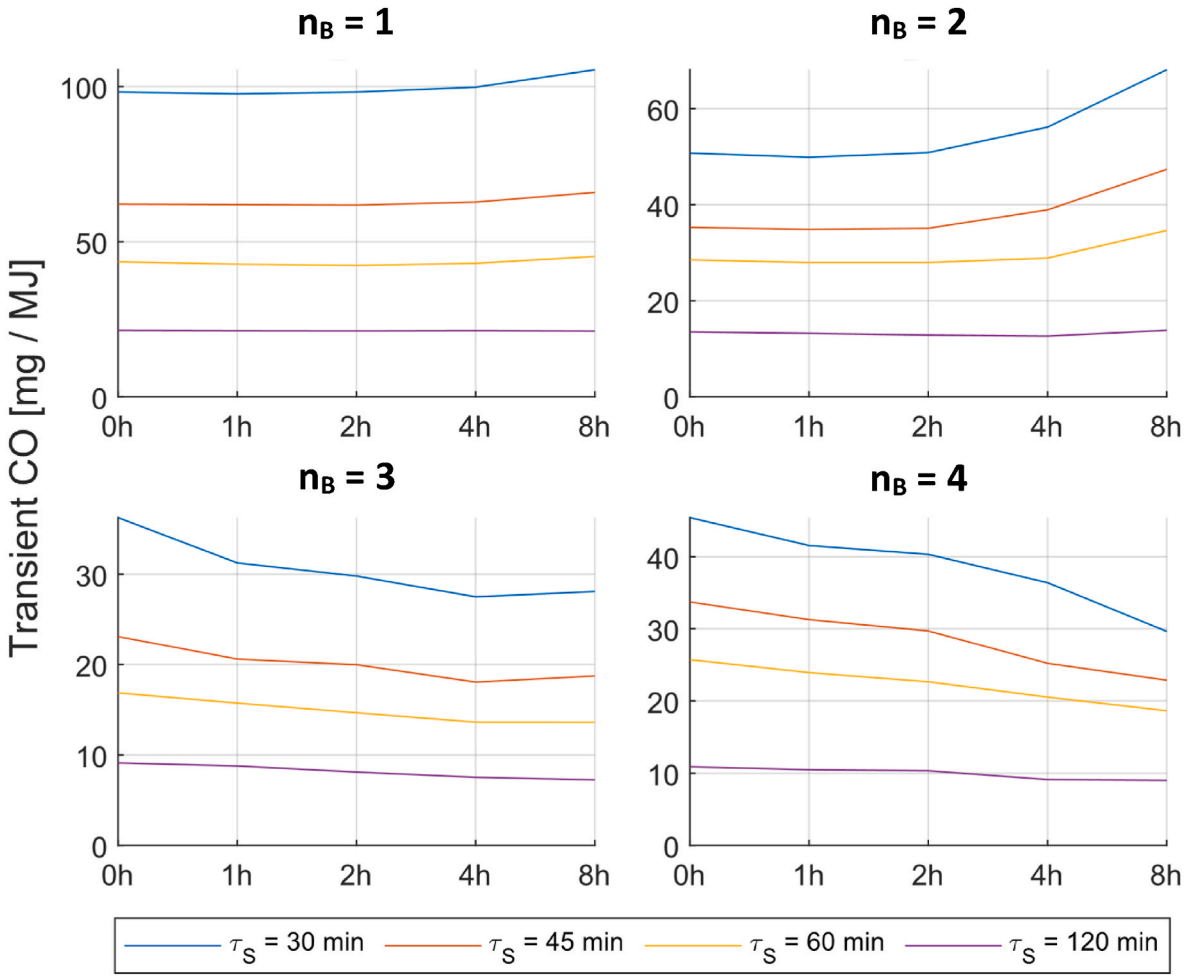


**Fig. 16.** Impact of mitigating demand peaks with different smoothing intervals on the annual transient CO emissions of wood heating plants with one to four wood boilers, a fossil auxiliary boiler and a boiler output range of 50%.

boilers with heat output of more than 500 kW are considered, which are commonly equipped with electrostatic precipitators. In addition, a distinction is made according to four different operating states, i.e. stationary operation at full load and part load and transient phases during startups and shutdowns. The emissions of the fossil fuel auxiliary boilers were calculated with averaged emission factors that represent the boiler operation in the different operation states. The annual emission factor $\varepsilon_{a,k}$ of the pollutant $k$ is calculated by (37). The numerator represents the absolute annual emission calculated by the annual time integral of the emission rate. The emission rate is calculated by the multiplication of boiler input power $\dot{Q}_{B,in,i}$ and the emission factor $EF_k$ of the pollutant $k$. The emission factors depend on the time as different emission factors are used for different boiler operation states. The annual absolute emission is divided by the annual heat demand of the district heating network.

$$\varepsilon_{a,k} = \frac{\int_{t_0}^{t_0+\tau_a} \sum_{i=1}^{n_K} \dot{Q}_{B,in,i}(t) \bullet EF_k(t) dt}{\int_{t_0}^{t_0+\tau_a} \dot{Q}_D(t)\, dt} \tag{37}$$

## 3. Model validation and verification

### 3.1. Model validation

The model is validated using measurement data from a test plant. The test plant consists of a 150 kW moving grate boiler and a 3030 L heat storage tank. In a first step, operating measurements are carried out with the test plant. Three validation measurements of 24 h each are carried out with typical heat demand profiles. In a second step, the test plant is modelled. A simulation is carried out with the same heat demand profiles. For validation, the measured data and the simulation data are compared. The deviations of the simulation results from the measured data are quantified in the Euclidean norm $\|x\|_2$ (38) and the max norm $\|x\|_{max}$ (39). The test plant is illustrated in Figs. 9 and 10.

$$\|x\|_2 = \frac{1}{n} \bullet \sqrt{\sum_{i=1}^{n} \left(x_{sim,i} - x_{meas,i}\right)^2} \tag{38}$$

$$\|x\|_{max} = \max\left(\left|x_{sim,i} - x_{meas,i}\right|\right) \tag{39}$$

Figs. 11 and 12 show the measured and the simulated system behavior for one of three validation measurements. Table 5 summarizes the error norms for all three measurements. Fig. 11 shows the measured and the simulated daily course of the boiler output. The simulation reproduces the daily curve of the measured boiler output accurately with an error norm of 3.3%. Fig. 12 shows the measured and simulated storage temperatures. The simulated temperatures reproduce the daily

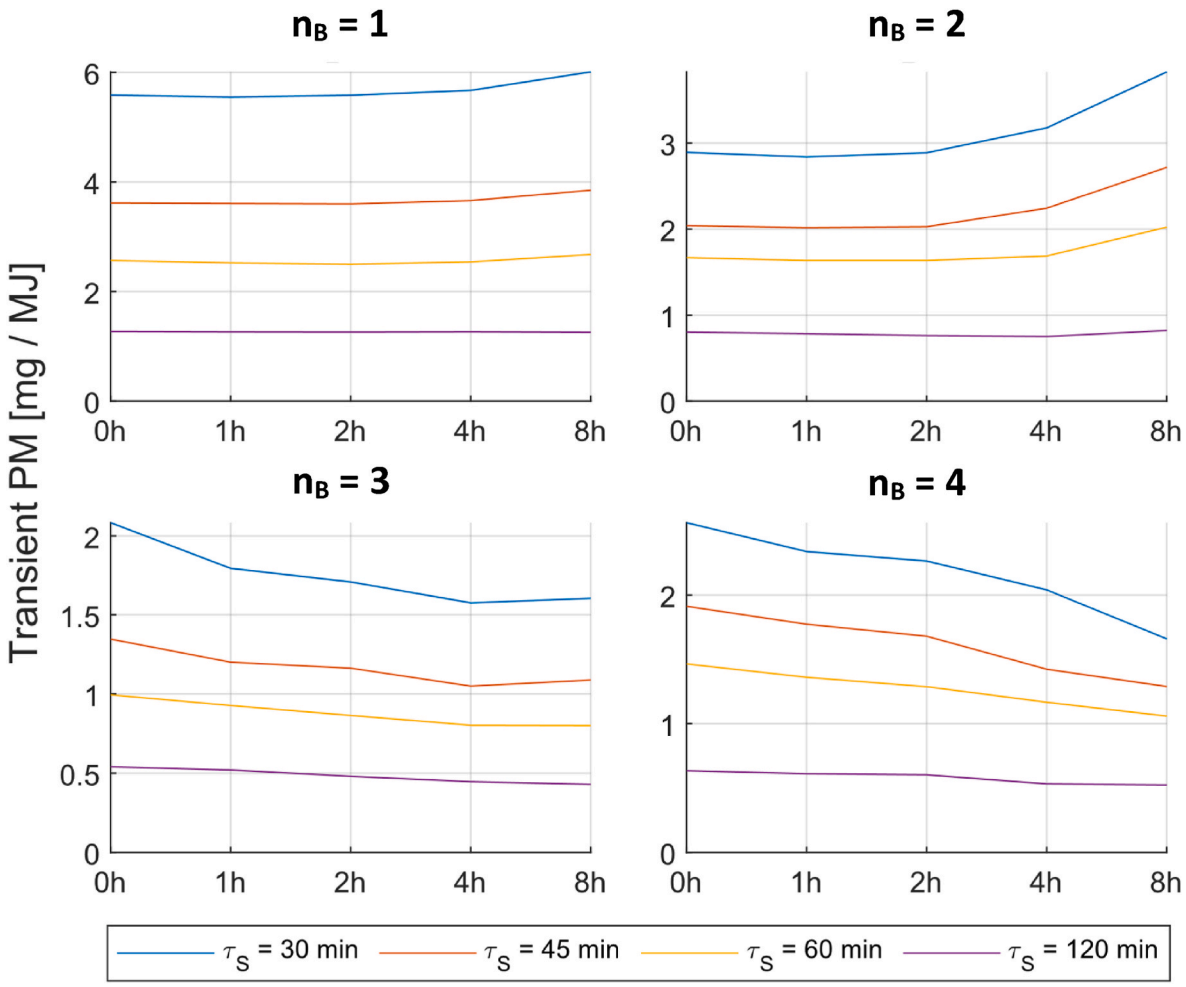


**Fig. 17.** Impact of mitigating demand peaks with different smoothing intervals on the annual transient PM emission of wood heating plants with one to four wood boilers, a fossil auxiliary boiler and a boiler output range of 50%.

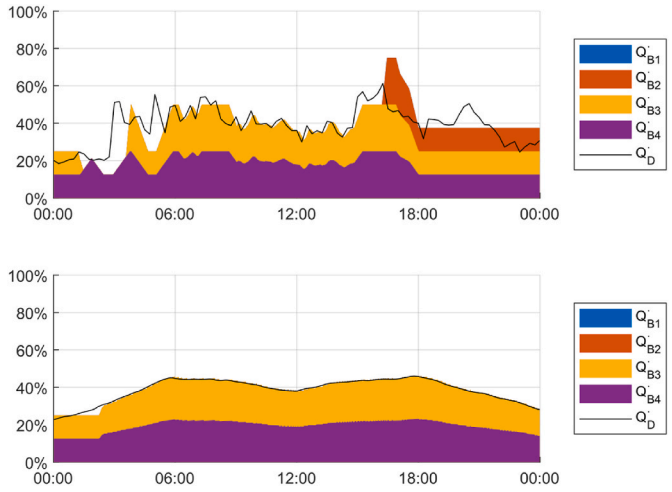


**Fig. 18.** Impact of mitigating demand peaks on the daily system operation for a wood heating plant with four wood boilers and a heat storage capacity of 60 min. The heat demand profile of the top figure is not filtered. The heat demand profile of the bottom figure is smoothed with an 8 h moving average. The heat example day represents a day with a medium heat demand.

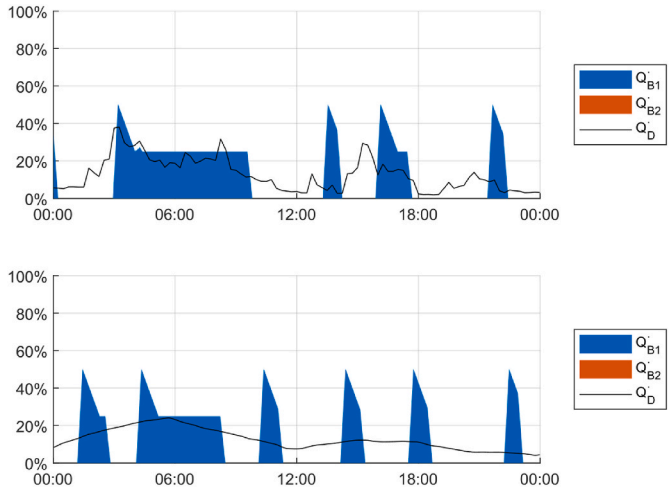


**Fig. 19.** Impact of mitigating demand peaks on the daily system operation for a wood heating plant with two wood boilers and a heat storage capacity of 60 min. The heat demand profile of the top figure is not filtered. The heat demand profile of the bottom figure is smoothed with an 8 h moving average. The heat example day represents a day with a low heat demand.

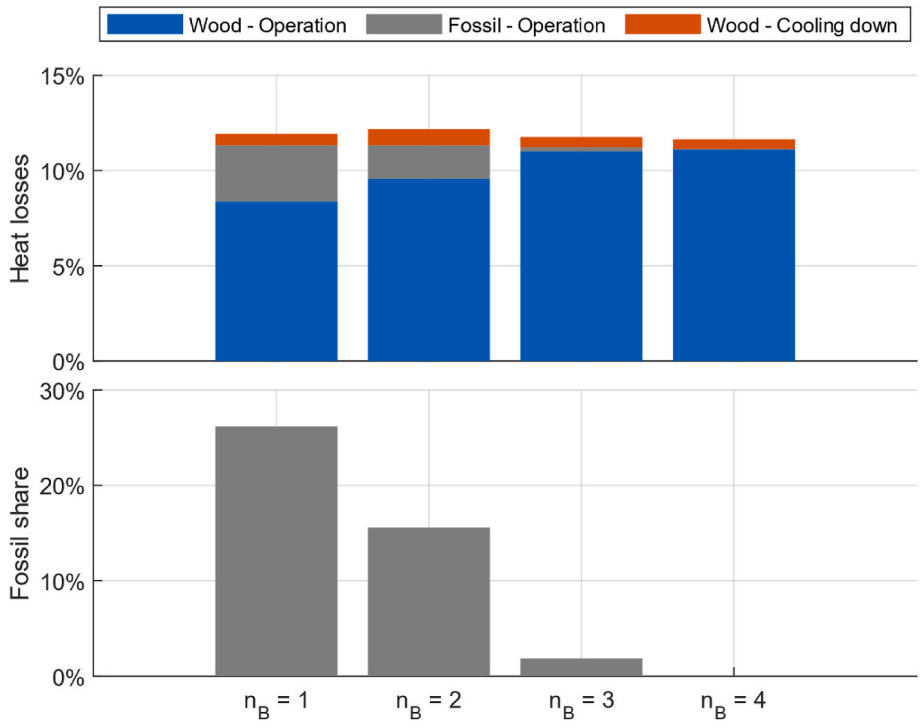


**Fig. 20.** Annual heat losses of wood heating plants with one to four wood boilers, a fossil auxiliary boiler, a boiler output range of 50% and a heat storage of 1 h.

course of the measured storage temperatures accurately with an error norm of 2.3 K.

## 4. Results

### 4.1. Fossil share

Fig. 13 shows the annual share of fossil heat production for different plant configurations. The numerical data is given in Table 6. The fossil share is calculated by dividing the annual output of the fossil auxiliary boiler by the annual heat demand of the district heating network.

Single wood boilers without output modulation cycle heavily at low loads and have to be replaced with fossil-based boilers to reduce pollutant emissions. Plants with one wood boiler and without boiler output modulation show a fossil share of 95% and are not suitable for year-round operation. The cycling problems at low load can be reduced by smaller wood boilers in cascade or by boiler output modulation. Cascade systems without boiler output modulation cause a fossil share of 27% in case of two wood boilers and can be further reduced to 12% by use of four wood boilers. In a heating plant with a single wood boiler with a boiler output range of 50%, a fossil share of 26% is achieved. Consequently, the use of two boilers without output modulation and the use of one boiler with a 50% boiler output range have a similar effect on the annual fossil share. The use of two wood boilers with an output range of 50% reduces the fossil share to 15%, while three or four wood boilers reduce the fossil heat demand to close to zero. For a fossil-free operation, a boiler output range of more than 50% is a minimum requirement for cascade systems with three or four boilers. A boiler output range of at least 70% (i.e. from 30% to 100%) is required for two-boiler systems, and approximately 90% boiler output range is needed for single-boiler systems.

### 4.2. Pollutant emissions

Fig. 14 shows the annual pollutant emissions in relation to the produced heat for different plant configurations with boiler ouput ranges of 50%. As an aid to interpretation, the fossil share of the annual heat supplied is shown additionally.

In the top diagram it can be observed that the CO emissions are mainly caused by the wood boilers. The fossil auxiliary boilers only contribute e.g. 4% in case of a single wood boiler system with a fossil share of 26%. Between 45% and 74% of the CO emissions from the wood boilers are caused from stationary operation. The remaining 26%–55% result from start-up and shut-down phases, which cause increased CO emissions. This part of the emissions can be decreased by avoiding startups and shutdowns of the wood boilers. As the number of boilers increases, the CO emissions increase due to the decrease of the fossil share. In the single wood boiler system, more than 25% of the heat demand is covered by the fossil fuel auxiliary boiler. Thus, the annual output of the wood boiler is lowered and so are its CO emissions. In a system with four boilers, no additional fossil energy is required. The wood boilers have a higher annual output and thus cause higher CO emissions. The single wood boiler system causes the highest CO emissions due to startup and shutdown processes. As the number of boilers increases, the CO emissions of the startup and shutdown processes decrease and reach a minimum for the system with three wood boilers. This system emits 60% less CO during the startup and shutdown processes than the single wood boiler system.

In the second diagram it can be observed that the PM emissions are also mainly caused by the wood boilers, while the fossil auxiliary boilers only contribute a negligible part. The PM emissions behave similar as the CO emissions. As the number of boilers increases, the emissions in stationary operation increase, which is due to the decreasing fossil share. Between 8% and 25% of PM emissions are caused during startup and shutdown. The PM emissions of the startup and shutdown processes decrease with increasing number of boilers and reach a minimum at three boilers.

The third diagram shows that 92%–98% of the $NO_X$ emissions are caused by the wood boilers in stationary operation. As the number of boilers increases, the $NO_X$ emissions in stationary operation increase, which is due to the decreasing fossil share. For single and two wood boiler systems, the fossil auxiliary boilers cause up to 8% of the $NO_X$ emissions.

The lowest diagram shows that the fossil share and therefore the

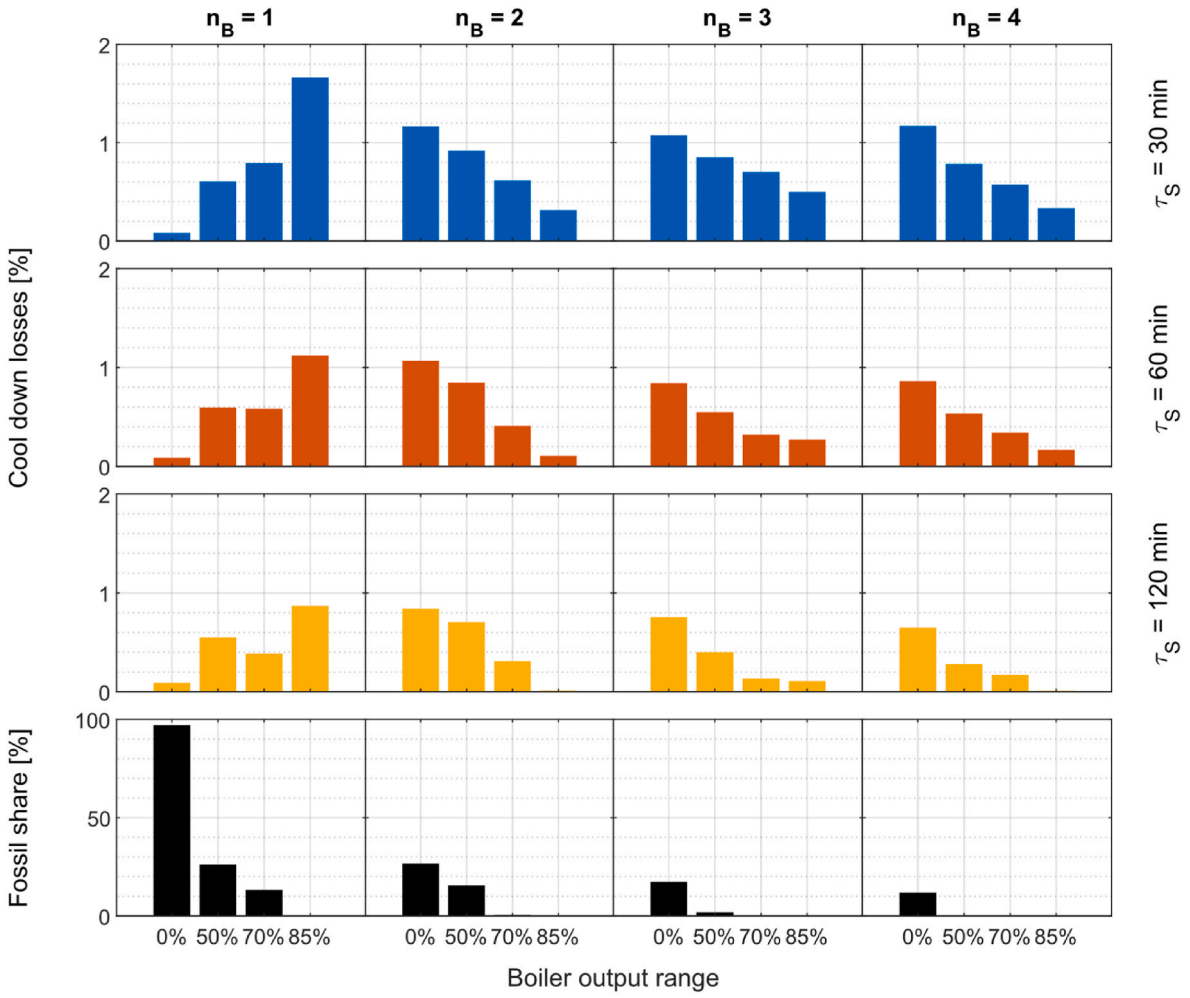


**Fig. 21.** Annual cool down losses of wood heating plants with one to four wood boilers and a fossil auxiliary boiler.

fossil $CO_2$ emissions decrease with increasing number of wood boilers. Only in systems with four boilers, no non-renewable $CO_2$ is emitted as no additional fossil heat is needed.

The previous graph showed that the CO, PM and $NO_X$ emissions of the stationary boiler operation are inversely proportional to the fossil share and that the startup and shutdown processes cause a noticeable share of the CO and PM emissions. Since a low fossil share is desired, the pollutant emissions in stationary operation can only be reduced by an optimal combustion control, while the pollutant emissions of the startup and shutdown processes are determined by the annual number of startup and shutdown processes. The annual number of startup and shutdown operations depends on the number of boilers, the heat storage capacity and the boiler output range. Fig. 15 shows the CO and PM emissions of the startup and shutdown operations different plant configurations in the upper six diagrams. The two bottom diagrams show the fossil share and the non-renewable $CO_2$ emissions comprising the whole year and not only the startup and shutdown operations.

For systems with more than one wood boiler, CO and PM emissions from startup and shutdown operations decrease with increasing boiler output range. Systems with a boiler output range of 50% cause less than half the emissions during startup and shutdown operations of systems without boiler output control. By increasing the boiler output range to 70% or 85%, the emissions of the startup and shutdown operations are further reduced. The annual CO and PM emissions from startup and shutdown operation decrease with increasing heat storage capacity. A plant with a 60 min storage capacity produces less than half the emissions of a plant with a 30 min storage capacity. By doubling the capacity from 60 to 120 min, CO and PM emissions from startup and shutdown operation can be further reduced but not halved. The startup and shutdown of the single boiler system cause less CO and PM emissions than systems with two or more wood boilers. This can be explained by the low annual output of the wood boiler in the single wood boiler system. The low annual output is reflected in the high fossil share and thus in the high $CO_2$ emissions. A system with three wood boilers causes less CO and PM emissions in the startup and shutdown processes than a system with two wood boilers. The CO and PM emissions of the startup and shutdown processes of a four wood boiler system are slightly higher than those of a system with three wood boilers, while the $CO_2$ emissions are slightly reduced from a low level to zero. The $CO_2$ emissions behave linearly to the fossil share and decrease with increasing boiler output range and increasing number of boilers. The storage capacity has only minor influence on the fossil share and the fossil $CO_2$ emissions.

Figs. 16 and 17 show the impact of mitigating demand peaks with different smoothing intervals on the annual transient CO and PM emissions of different plant configurations boiler output ranges of 50%. It can be observed that mitigating demand peaks has an influence on the transient pollutant emissions. The influence is more pronounced for wood heating plants with small heat storage capacity. Mitigating demand peaks can lead to both an increase and a reduction of the transient CO and PM emissions. When the heat demand is high, smoothing the load peaks can prevent boiler startups and shutdowns (Fig. 18). At low heat demand, on the other hand, additional boiler startups and shutdowns can occur (Fig. 19). In wood heating plants with up to two wood boilers, the increase in boiler starts at low heat demand predominates,

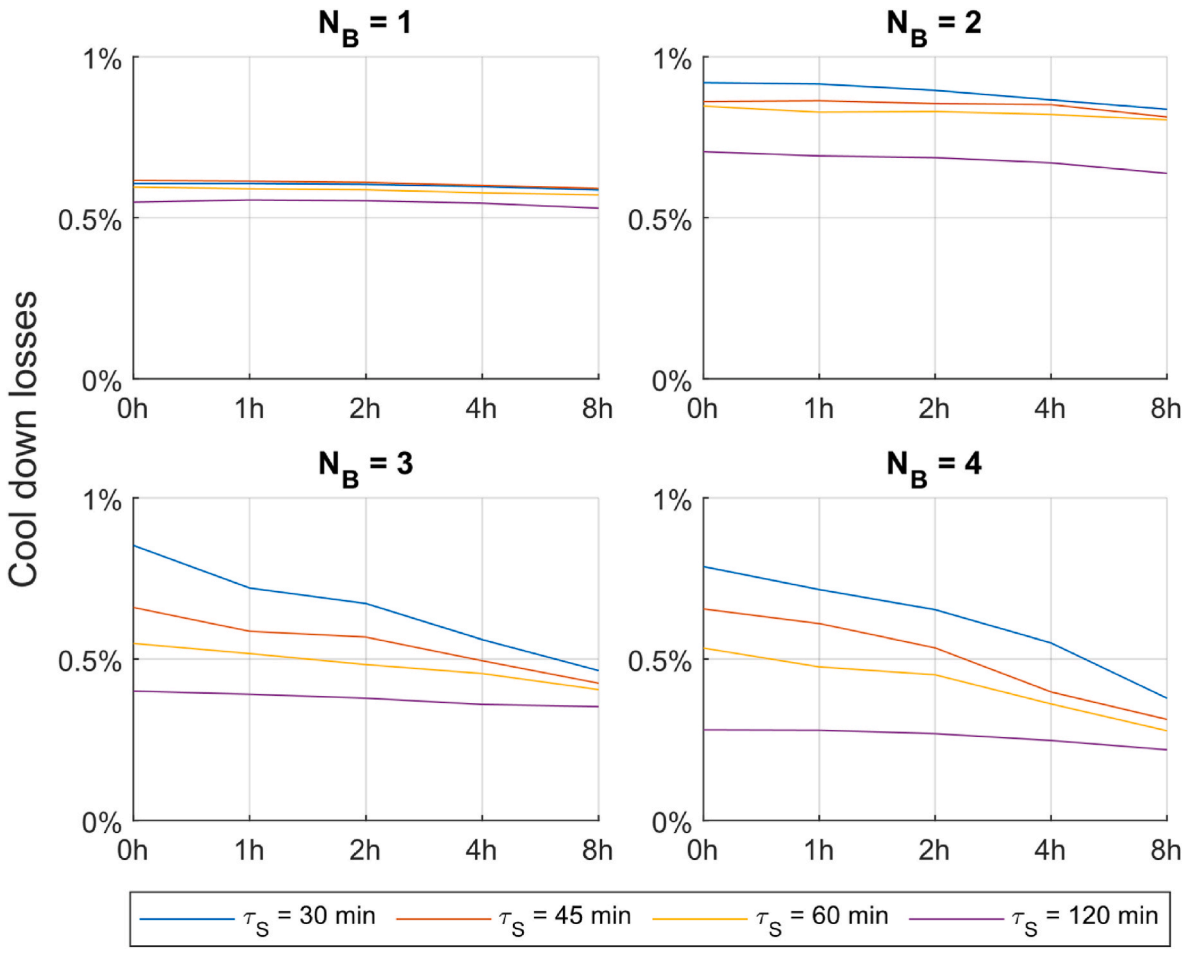


**Fig. 22.** Impact of mitigating demand peaks with different smoothing intervals on the annual cool down losses of wood heating plants with one to four wood boilers, a fossil auxiliary boiler and a boiler output range of 50%.

which leads to an increase in emissions due to mitigating demand peaks. In plants with more than two wood boilers, the reduction of boiler starts at high heat demand predominates, which leads to a reduction of pollutant emissions by mitigating demand peaks.

### 4.3. Heat losses

Fig. 20 shows the annual heat losses of different plant configurations. The graph distinguishes between heat losses from the stationary operation of the wood boilers, the heat losses from the operation of the fossil auxiliary boiler and the cooling down losses of the wood boilers that occur after a boiler shut down. The cooling down losses of the fossil auxiliary boiler are not considered. As an aid to interpretation, the fossil share of the annual heat is also shown. The main part of the heat losses occurs in the stationary operation of the wood boilers and the fossil boilers. The sum of the heat losses from the stationary operation of the wood boilers and the fossil auxiliary boiler hardly depends on the number of wood boilers. As the number of wood boilers increases, the fossil share and thus also the heat losses from the fossil boilers decrease while the heat losses from the stationary operation of the wood boilers increase. The cooling losses of the wood boilers account for between 4% and 6% of the heat losses in the systems considered. More cooling losses occur in the two wood boiler system than in the single wood boiler system. From two wood boilers upwards, the cooling losses decrease with increasing number of boilers.

By analyzing the previous graph, it was possible to show that the annual cooling losses of the wood boilers depend on the number of boilers. Fig. 21 shows the cooling losses of different plant configurations in the upper three diagrams. The lowest diagram shows the fossil share. The cooling losses of systems without a fossil share amount up to 1.7% of the annual heat production, which corresponds to 13% of the total annual heat losses. For systems with more than one wood boiler, the cooling losses decrease with increasing boiler output range. For the single wood boiler system, the cooling losses increase with increasing boiler output range, which is due to the increase in the fossil share. The single wood boiler system with a boiler output range of 85% causes the highest cooling losses. The cooling losses decrease with increasing storage capacity.

Fig. 22 shows the impact of mitigating demand peaks with different smoothing intervals on the annual cool down losses of wood heating plants with a boiler output range of 50%. A smoothing of the load curve simplifies the control of wood boilers and therefore prevents unnecessary switching on and off of wood boilers. The lower number of boiler starts consequently leads to lower cooling losses. The effect is only weakly pronounced in systems with a large storage capacity, since the peaks in demand can be covered by the stored heat. For systems with one boiler, the effect is hardly recognizable, since the wood boiler is replaced by the fossil auxiliary boiler at low loads in summer, which prevents many boiler starts.

### 4.4. Summary of all results

Table 6 shows the share of fossil fuels contributing to the total heat demand as function of the boiler output range of the wood boiler and the number of wood boilers. The system configurations with a predicted fossil share of 0% (green area) enable a fossil-free heat production all

**Table 7**
Numerical results of the pollutant emissions and the heat losses.

| Number of boilers | Boiler output range | Storage capacity | Fossil share | CO | | PM | | $NO_X$ | | $CO_2$ | | Heat losses | | |
|---|---|---|---|---|---|---|---|---|---|---|---|---|---|---|
| | | | | TransientOperation | StationaryOperation | TransientOperation | StationaryOperation | TransientOperation | StationaryOperation | Natural gas | Light fuel oil | Operation | Cool down | Fossil |
| [−] | [%] | [min] | [%] | [mg/MJ] | | | | | | [g/MJ] | | [%] | | |
| 1 | 0 | 30 | 97.0 | 7.9 | 1.2 | 0.4 | 0.3 | 1.4 | 3.3 | 54.4 | 75.1 | 0.4 | 0.1 | 11.2 |
| | | 60 | 97.0 | 5.4 | 1.3 | 0.3 | 0.3 | 0.9 | 3.7 | 54.4 | 75.1 | 0.4 | 0.1 | 11.6 |
| | | 120 | 97.0 | 3.4 | 1.4 | 0.2 | 0.3 | 0.6 | 3.9 | 54.4 | 75.1 | 0.4 | 0.1 | 11.3 |
| | 50 | 30 | 25.9 | 98.3 | 32.9 | 5.6 | 7.2 | 18.5 | 90.3 | 14.5 | 20.0 | 8.4 | 0.6 | 2.9 |
| | | 60 | 26.2 | 43.5 | 35.6 | 2.6 | 7.8 | 8.7 | 97.9 | 14.7 | 20.3 | 8.4 | 0.6 | 3.0 |
| | | 120 | 25.1 | 21.4 | 36.8 | 1.3 | 8.1 | 4.3 | 101.0 | 14.1 | 19.4 | 8.4 | 0.5 | 2.8 |
| | 70 | 30 | 14.9 | 85.0 | 45.4 | 4.8 | 6.8 | 15.8 | 104.3 | 8.4 | 11.5 | 9.8 | 0.8 | 1.7 |
| | | 60 | 13.2 | 24.8 | 50.7 | 1.5 | 6.6 | 5.1 | 110.1 | 7.4 | 10.2 | 9.8 | 0.6 | 1.5 |
| | | 120 | 12.7 | 7.9 | 53.1 | 0.5 | 6.2 | 1.7 | 110.9 | 7.2 | 9.9 | 9.8 | 0.4 | 1.4 |
| | 85 | 30 | 0.1 | 103.1 | 52.2 | 5.7 | 7.3 | 18.7 | 116.6 | 0.0 | 0.1 | 11.1 | 1.7 | 0.0 |
| | | 60 | 0.1 | 24.8 | 58.6 | 1.5 | 7.2 | 5.0 | 124.4 | 0.0 | 0.1 | 11.1 | 1.1 | 0.0 |
| | | 120 | 0.1 | 10.4 | 60.1 | 0.7 | 7.0 | 2.5 | 125.5 | 0.0 | 0.0 | 11.1 | 0.9 | 0.0 |
| 2 | 0 | 30 | 26.3 | 120.4 | 31.5 | 6.5 | 6.9 | 21.0 | 86.5 | 14.7 | 20.3 | 8.2 | 1.2 | 2.9 |
| | | 60 | 26.6 | 68.2 | 34.1 | 3.7 | 7.5 | 11.9 | 93.5 | 15.0 | 20.6 | 8.2 | 1.1 | 3.0 |
| | | 120 | 26.5 | 35.6 | 35.6 | 1.9 | 7.8 | 6.2 | 97.9 | 14.8 | 20.5 | 8.2 | 0.8 | 3.0 |
| | 50 | 30 | 15.3 | 50.8 | 40.8 | 2.9 | 9.0 | 9.6 | 112.0 | 8.6 | 11.9 | 9.6 | 0.9 | 1.7 |
| | | 60 | 15.6 | 28.5 | 41.9 | 1.7 | 9.2 | 5.6 | 115.1 | 8.7 | 12.0 | 9.6 | 0.8 | 1.8 |
| | | 120 | 15.6 | 13.5 | 42.7 | 0.8 | 9.4 | 2.7 | 117.2 | 8.7 | 12.1 | 9.6 | 0.7 | 1.8 |
| | 70 | 30 | 0.4 | 27.9 | 54.7 | 1.6 | 8.6 | 5.4 | 128.1 | 0.3 | 0.3 | 11.1 | 0.6 | 0.1 |
| | | 60 | 0.5 | 12.0 | 56.6 | 0.7 | 8.3 | 2.5 | 129.2 | 0.3 | 0.4 | 11.1 | 0.4 | 0.1 |
| | | 120 | 0.4 | 6.2 | 57.7 | 0.4 | 8.1 | 1.4 | 129.1 | 0.2 | 0.3 | 11.1 | 0.3 | 0.0 |
| | 85 | 30 | 0.0 | 14.2 | 58.4 | 0.8 | 7.6 | 2.8 | 127.0 | 0.0 | 0.0 | 11.1 | 0.3 | 0.0 |
| | | 60 | 0.0 | 3.1 | 59.2 | 0.2 | 7.7 | 0.7 | 128.4 | 0.0 | 0.0 | 11.1 | 0.1 | 0.0 |
| | | 120 | 0.0 | 0.1 | 59.5 | 0.0 | 7.7 | 0.0 | 128.7 | 0.0 | 0.0 | 11.1 | 0.0 | 0.0 |
| 3 | 0 | 30 | 17.0 | 115.8 | 36.6 | 6.2 | 8.1 | 20.2 | 100.7 | 9.5 | 13.1 | 9.3 | 1.1 | 1.9 |
| | | 60 | 17.4 | 54.0 | 39.7 | 2.9 | 8.7 | 9.4 | 108.9 | 9.7 | 13.5 | 9.3 | 0.8 | 2.0 |
| | | 120 | 17.1 | 32.3 | 40.7 | 1.7 | 9.0 | 5.6 | 111.8 | 9.6 | 13.3 | 9.3 | 0.8 | 1.9 |
| | 50 | 30 | 1.9 | 36.3 | 48.1 | 2.1 | 10.6 | 7.0 | 132.0 | 1.1 | 1.5 | 11.0 | 0.9 | 0.2 |
| | | 60 | 1.9 | 16.9 | 49.0 | 1.0 | 10.8 | 3.4 | 134.7 | 1.0 | 1.4 | 11.0 | 0.5 | 0.2 |
| | | 120 | 1.8 | 9.1 | 49.4 | 0.5 | 10.9 | 1.8 | 135.8 | 1.0 | 1.4 | 11.0 | 0.4 | 0.2 |
| | 70 | 30 | 0.0 | 25.3 | 54.5 | 1.5 | 8.7 | 4.9 | 129.0 | 0.0 | 0.0 | 11.1 | 0.7 | 0.0 |
| | | 60 | 0.0 | 7.4 | 55.0 | 0.5 | 9.1 | 1.6 | 132.0 | 0.0 | 0.0 | 11.1 | 0.3 | 0.0 |
| | | 120 | 0.0 | 3.1 | 56.2 | 0.2 | 8.8 | 0.7 | 131.6 | 0.0 | 0.0 | 11.1 | 0.1 | 0.0 |
| | 85 | 30 | 0.0 | 15.9 | 57.3 | 0.9 | 8.0 | 3.1 | 127.8 | 0.0 | 0.0 | 11.1 | 0.5 | 0.0 |
| | | 60 | 0.0 | 3.6 | 55.4 | 0.2 | 9.1 | 0.8 | 132.3 | 0.0 | 0.0 | 11.1 | 0.3 | 0.0 |
| | | 120 | 0.0 | 0.8 | 56.0 | 0.1 | 8.9 | 0.2 | 132.3 | 0.0 | 0.0 | 11.1 | 0.1 | 0.0 |
| 4 | 0 | 30 | 11.9 | 114.2 | 39.3 | 6.1 | 8.7 | 19.9 | 108.0 | 6.7 | 9.2 | 9.9 | 1.2 | 1.3 |
| | | 60 | 11.8 | 61.5 | 41.9 | 3.3 | 9.2 | 10.7 | 115.1 | 6.6 | 9.2 | 9.9 | 0.9 | 1.3 |
| | | 120 | 11.9 | 38.0 | 43.0 | 2.0 | 9.5 | 6.6 | 118.2 | 6.7 | 9.2 | 9.9 | 0.7 | 1.3 |
| | 50 | 30 | 0.0 | 45.4 | 48.1 | 2.6 | 10.6 | 8.5 | 132.2 | 0.0 | 0.0 | 11.1 | 0.8 | 0.0 |
| | | 60 | 0.0 | 25.7 | 49.1 | 1.5 | 10.8 | 4.9 | 134.9 | 0.0 | 0.0 | 11.1 | 0.5 | 0.0 |
| | | 120 | 0.0 | 10.9 | 49.9 | 0.6 | 11.0 | 2.1 | 137.0 | 0.0 | 0.0 | 11.1 | 0.3 | 0.0 |
| | 70 | 30 | 0.0 | 29.9 | 53.9 | 1.7 | 8.9 | 5.7 | 128.9 | 0.0 | 0.0 | 11.1 | 0.6 | 0.0 |
| | | 60 | 0.0 | 14.2 | 54.9 | 0.8 | 8.9 | 2.7 | 130.8 | 0.0 | 0.0 | 11.1 | 0.3 | 0.0 |
| | | 120 | 0.0 | 3.8 | 56.3 | 0.2 | 8.7 | 0.8 | 131.3 | 0.0 | 0.0 | 11.1 | 0.2 | 0.0 |
| | 85 | 30 | 0.0 | 15.9 | 55.7 | 0.9 | 8.6 | 3.1 | 129.6 | 0.0 | 0.0 | 11.1 | 0.3 | 0.0 |
| | | 60 | 0.0 | 4.8 | 56.8 | 0.3 | 8.5 | 1.0 | 130.6 | 0.0 | 0.0 | 11.1 | 0.2 | 0.0 |
| | | 120 | 0.0 | 0.1 | 57.7 | 0.0 | 8.3 | 0.0 | 130.7 | 0.0 | 0.0 | 11.1 | 0.0 | 0.0 |

year round in compliance with the condition for minimum load operation of wood boilers. Table 7 summarizes the results of the pollutant emissions and the heat losses for the investigated system configurations.

## 5. Conclusions

The simulation investigates the behavior of heating plants with one to four wood boilers combined with an auxiliary fossil fuel boiler and a heat storage tank. In addition, a low load condition for the operation of the wood boilers is considered which requires minimum 12 h operation of one wood boiler per day to avoid frequent startups and shutdowns. The results demonstrate how the use of auxiliary fossil heat, the pollutant emissions and the heat losses in wood heating plants can be reduced. The study investigates mitigating of heat demand peaks, increasing the heat storage capacity, expanding the output range of the wood boilers and increasing the number of wood boilers in the heating plant. Due to the low load condition, a fossil share of the investigated wood heating plants amounts between 0% and a theoretical value of 97%. The fossil share, the transient fraction of the pollutant emissions and the cool down losses can be reduced through optimized design and operation of the heating plant. For operation without additional fossil heat, the boilers in a wood-fired heating plant must be able to provide low heat outputs for periods with a low heat demand. Low heat outputs can be achieved by a large boiler output range of the wood boilers or by installing several smaller wood boilers instead of one large boiler. In terms of the annual fossil share, both solutions are target oriented. For a heating plant with one single wood boiler and a heat storage capacity of 1 h at nominal load, a continuous boiler operation from approximately 15%–100% of the nominal boiler output would be necessary to meet the low load condition all year long. For heating plants with two, three or four wood boilers, a minimum boiler output of 30%, 40% and 60% is needed. For all heating plants, an increase in storage capacity leads to a reduction in annual CO and PM emissions. The annual CO and PM emissions of the regarded fossil-free heating plants were reduced by 17% and 8% respectively by doubling the heat storage capacity from 30 to 60 min of the nominal boiler output. A further doubling of the heat storage capacity from 60 to 120 min reduces the annual CO and PM emissions by 9% and 6%. The annual heat losses are reduced by 1% by doubling the heat storage capacity. Mitigating the heat demand peaks reduces the transient pollutant emissions and the cooling losses in systems with more than two wood boilers but can have a negative effect on the transient pollutant emissions for plants with one or two wood boilers.

## Credit author statement

Felix Schumacher; Term, Conceptualization, Methodology, Software, Programming, Verification, Validation, Writing, Visualisation; Dr. Prof. Thomas Nussbaumer, Term, Conceptualization, Supervision, Project Administration.

## Declaration of competing interest

The authors declare that they have no known competing financial interests or personal relationships that could have appeared to influence the work reported in this paper.

## Data availability

The authors do not have permission to share data.

## Acknowledgements

The study was supported by the Swiss Federal Office of Energy. The companies Allotherm AG, Heitzmann AG, Liebi LNC AG and Schmid AG energy solutions enabled the measurements at practical plants. Holzenergie Schweiz, Holzfeuerungen Schweiz and Energie Ausserschwyz AG supported the project evaluation in the accompanying group.

## Appendix A. Supplementary data

Supplementary data to this article can be found online at https://doi.org/10.1016/j.energy.2023.127596.

## References

[1] Vandermeulen A, van der Heijde B, Helsen L. Controlling district heating and cooling networks to unlock flexibility: a review. Energy 2018;151:103–15.
[2] Iea IEA. Heating report 2021. 2021.
[3] Werner S. International review of district heating and cooling. Energy; 2017.
[4] Johansson LS, et al. Particle emissions from biomass combustion in small combustors. Biomass Bioenergy 2003;25(4):435–46.
[5] Lillieblad L, et al. Boiler operation influence on the emissions of submicrometer-sized particles and polycyclic aromatic hydrocarbons from biomass-fired grate boilers. Energy Fuel 2004;18(2):410–7.
[6] Mermoud F, et al. Impact of load variations on wood boiler efficiency and emissions: in-situ monitoring of two boilers (2 MW and 0.65 MW) supplying a district heating system. Archives des sciences 2015;68:27–38.
[7] Win KM, Persson T, Bales C. Particles and gaseous emissions from realistic operation of residential wood pellet heating systems. Atmos Environ 2012;59:320–7.
[8] Good J, Nussbaumer T. Emissionsfaktoren moderner pelletkessel unter typischen heizbedingungen. Berne, Switzerland: Swiss Federal Office of Energy; 2009.
[9] Win KM, Persson T. Emissions from residential wood pellet boilers and stove characterized into start-up, steady operation, and stop emissions. Energy Fuel 2014;28(4):2496–505.
[10] Ghafghazi S, et al. Particulate matter emissions from combustion of wood in district heating applications. Renewable Sustainable Energy Rev 2011;15(6):3019–28.
[11] Nussbaumer T, Lauber A. Monitoring the availability of electrostatic precipitators (ESP) in automated biomass combustion plants. Biomass Bioenergy 2016;89:24–30.
[12] Singh R, Shukla A. A review on methods of flue gas cleaning from combustion of biomass. Renew Sustain Energy Rev 2014;29:854–64.
[13] Good J, et al. Methods for efficiency determination for biomass heating plants and influence of operation mode on plant efficiency. 2004.
[14] Haller MY, et al. A unified model for the simulation of oil, gas and biomass space heating boilers for energy estimating purposes. Part I: model development. Journal of Building Performance Simulation 2011;4(1):1–18.
[15] Strehler A. Technologies of wood combustion. Ecol Eng 2000;16:S25–40.
[16] Heinz A, et al. Fortschrittliche wärmespeicher zur erhöhung von solarem deckungsgrad und kesselnutzungsgrad sowie emissionsverringerung durch verringertes takten. Graz, Austria: Technische Universität Graz, Institut für Wärmetechnik; 2006.
[17] Wang K, et al. Thermal energy storage tank sizing for biomass boiler heating systems using process dynamic simulation. Energy Build 2018;175:199–207.
[18] Wang K, et al. Emissions from in-use residential wood pellet boilers and potential emissions savings using thermal storage. Sci Total Environ 2019;676:564–76.
[19] Butcher TA, Trojanowski R. Effect of thermal storage on the emissions and efficiency performance of a wood-pellet-fired residential boiler. ACS Omega 2020;5(44):28517–28.
[20] Guelpa E, Verda V. Demand response and other demand side management techniques for district heating: a review. Energy 2021;219:119440.
[21] Nussbaumer T, et al. Holzkessel kaskadenanlagen mit speicher (hokaspe). 2022.
[22] Schumacher F, Good J, Nussbaumer T. In: Modellierung von Holzheizung, Wärmespeicher und Fernwärmenetz, vol. 16. Holzenergie-Symposium; 2020.
[23] Dittmar R. Advanced process control : PID-basisregelungen, vermaschte regelungsstrukturen, softsensoren, model predictive control. Walter de Gruyter GmbH & Co KG; 2017.
[24] Heinrich B. Grundlagen regelungstechnik: einfache übungen, praktische beispiele und komplexe aufgaben. Springer-Verlag; 2019.
[25] Good J, et al. Planungshandbuch QM holzheizwerke. CARMEN; 2022.
[26] Hellwig M. Entwicklung und anwendung parametrisierter standard-lastprofile. Technische Universität München; 2003.
[27] Nussbaumer T, et al. Handbook on planning of district heating networks. 2020.
[28] Haller M, et al. A unified model for the simulation of oil, gas and biomass space heating boilers for energy estimating purposes. Part II: parameterization and comparison with measurements. Journal of Building Performance Simulation 2011;4(1):19–36.
[29] Din DINEN. 303-5: heating boilers - Part 5: heating boilers for solid fuels, manually and automatically stoked, nominal heat output of up to 500 kW - terminology, requirements, testing and marking. 2018.
[30] Zotter P, Nussbaumer T. Aktualisierung Emissionsmodell Holzfeuerungen 2020: 2021.
[31] UVEK. Faktenblatt emissionsfaktoren feuerungen. 2015.